ASTROPHYS.J. 671 (2007) 1640
Preprint typeset using LaTeX style emulateapj v. 04/21/05

arXiv:0707.3144v2 [astro-ph] 26 Nov 2007

THE DISTANCES TO OPEN CLUSTERS FROM MAIN-SEQUENCE FITTING. IV. GALACTIC CEPHEIDS, THE LMC, AND THE LOCAL DISTANCE SCALE

DEOKKEUN AN, DONALD M. TERNDRUP, AND MARC H. PINSONNEAULT
Department of Astronomy, Ohio State University, 140 West 18th Avenue, Columbus, OH 43210;
deokkeun,terndrup,pinsono@astronomy.ohio-state.edu
Astrophys.J. 671 (2007) 1640

ABSTRACT

We derive the basic properties of seven Galactic open clusters containing Cepheids and construct their period-luminosity (*P-L*) relations. For our cluster main-sequence fitting we extend previous Hyades-based empirical color-temperature corrections to hotter stars using the Pleiades as a template. We use BVI_CJHK_s data to test the reddening law and include metallicity effects to perform a more comprehensive study for our clusters than prior efforts. The ratio of total to selective extinction R_V that we derive is consistent with expectations. Assuming the LMC *P-L* slopes, we find $\langle M_V \rangle = -3.93 \pm 0.07$ (statistical) ± 0.14 (systematic) for 10-day period Cepheids, which is generally fainter than those in previous studies. Our results are consistent with recent *HST* and *Hipparcos* parallax studies when using the Wesenheit magnitudes $W(VI)$. Uncertainties in reddening and metallicity are the major remaining sources of error in the *V*-band *P-L* relation, but a higher precision could be obtained with deeper optical and near-infrared cluster photometry. We derive distances to NGC 4258, the LMC, and M33 of $(m-M)_0 = 29.28 \pm 0.10$, 18.34 ± 0.06, and 24.55 ± 0.28, respectively, with an additional systematic error of 0.16 mag in the *P-L* relations. The distance to NGC 4258 is in good agreement with the geometric distance derived from water masers [$\Delta(m-M)_0 = 0.01 \pm 0.24$], our value for M33 is less consistent with the distance from an eclipsing binary [$\Delta(m-M)_0 = 0.37 \pm 0.34$], and our LMC distance is moderately shorter than the adopted distance in the *HST* Key Project, which formally implies an increase in the Hubble constant of $7\% \pm 8\%$.

Subject headings: Cepheids — distance scale — galaxies: individual (M33, NGC 4258) — Magellanic Clouds — open clusters and associations: general — stars: distances

1. INTRODUCTION

The Cepheid period-luminosity (*P-L*) relation has played a key role in the determination of distances within the Local Group and to nearby galaxies. By extension, it is also crucial for the calibration of secondary distance indicators used to determine the Hubble constant: see, for example, the *Hubble Space Telescope (HST)* Key Project on the extragalactic distance scale (Freedman et al. 2001, hereafter *HST* Key Project) and the *HST* program for the luminosity calibration of Type Ia supernovae (SNe Ia) by means of Cepheids (Sandage et al. 2006). The cosmic distance scale was usually established by defining the *P-L* relations for Cepheids in the Large Magellanic Cloud (LMC) because of its numerous Cepheids, many of which have been discovered as a result of microlensing campaigns (e.g., Udalski et al. 1999a). Despite decades of effort, however, there have been persistent differences in the inferred LMC distance from different methods (see Benedict et al. 2002a), including ones involving the same basic calibrators such as RR Lyrae or Cepheid variables.

The Galactic *P-L* relationship, on the other hand, was traditionally established using open clusters and associations containing Cepheids (see Feast & Walker 1987; Feast 2003; Sandage & Tammann 2006). There is also a steadily growing body of parallax work from the *Hipparcos* mission (Feast & Catchpole 1997; Madore & Freedman 1998; Lanoix et al. 1999; Groenewegen & Oudmaijer 2000; van Leeuwen et al. 2007) and the *HST* (Benedict et al. 2002b, 2007), as well as distances derived from the Baade-Becker-Wesselink moving atmospheres method (Gieren et al. 1997, 1998, 2005) and interferometric angular diameter measurements (Lane et al. 2000, 2002; Kervella et al. 2004a,b). In the current paper we focus on the Cepheid distance scale as inferred from Galactic open clusters and its applications for the extragalactic distance scale.

There are strengths and weaknesses in all of the methods used to establish the Galactic Cepheid distance scale. The absolute calibration of the *P-L* relation requires not only accurate distance measurements but also appropriate accounting for the effects of interstellar extinction and reddening because Galactic Cepheids are heavily obscured with an average $E(B-V)$ of order 0.5 mag (Fernie 1990). Reddening can be inferred more precisely for clusters, while field Cepheids are more numerous. This difficulty can be partially overcome by the usage of the "reddening-free" or Wesenheit index (Freedman et al. 1991), but there are embedded assumptions about the extinction law even in such a system.

We believe that the time is right for a systematic reappraisal of the Cepheid distance scale as inferred from open clusters. Recent parallax work employing the Wesenheit index (Benedict et al. 2007; van Leeuwen et al. 2007) has yielded consistent claims of a somewhat smaller LMC distance modulus (≈ 18.40 mag) than the ones adopted by the *HST* Key Project (18.50 mag) or Sandage et al. program (18.54 mag). In addition, there are now independent geometric tests of distances to other galaxies, which have large numbers of Cepheids. These include massive eclipsing binaries in systems such as M31 (Ribas et al. 2005) and M33 (Bonanos et al. 2006) and astrophysical water masers in NGC 4258 (Herrnstein et al. 1999). As described below, the availability of both more complete data in various photometric passbands and better theoretical templates permits a more comprehensive look at the open cluster Cepheid distance scale, which can in turn be compared with the alternate methods described above. We can also use the open clusters with Cepheids to test our ability to

derive precise distances and reddenings to heavily obscured and poorly studied systems. We believe that the net result is a more secure and robust determination of the extragalactic distance scale.

We have been engaged in a long-term effort to create stellar evolution models with the latest input physics and to generate isochrones that are calibrated against photometry in local star clusters with accurate distances. After verifying that the models are in agreement with the physical parameters of binaries and single stars in the Hyades (Pinsonneault et al. 2003, 2004, hereafter Papers I and II, respectively), we developed a procedure for empirically correcting the color-effective temperature ($T_{\rm eff}$) relations to match photometry in the Hyades (Paper II). Isochrones generated in this way accurately reproduce the shapes of the main-sequence (MS) in several colors, allowing the determination of distances to nearby clusters to an accuracy of ~ 0.04 mag in distance modulus (or 2% in distance) (An et al. 2007, hereafter Paper III).

We extend the Hyades-based empirical corrections on theoretical isochrones using the Pleiades and apply our techniques to a set of Cepheid-bearing open clusters that have good multi-color photometry. Selection of cluster sample and compilation of cluster photometry are presented in § 2. Procedures on the isochrone calibration and MS-fitting method are described in § 3. New cluster distances and extinctions are presented in § 4. In § 5 we construct multi-wavelength Galactic *P-L* relations and discuss various systematic errors. In § 6 we estimate distances and reddenings for the maser galaxy NGC 4258, the LMC, and M33. We summarize our results in § 7 and discuss the importance of extinction corrections in the Cepheid distance scale.

2. CLUSTER AND CEPHEID DATA

2.1. *Cluster Selection, Metallicity, and Age*

About 30 open clusters and associations in the Galaxy are known to harbor Cepheid variables (Feast & Walker 1987; Feast 1999), but not all of these are useful for MS fitting because many are extremely sparse or poorly studied. We first excluded systems with overtone or double-mode Cepheids and then examined the available photoelectric and/or CCD photometry for each cluster. From visual inspection of color-magnitude diagrams (CMDs) we narrowed down the list to 10 promising candidates for MS fitting. The populous twin clusters *h*&χ Per were excluded from the current analysis because their young age introduces significant uncertainties in the isochrone calibration, and the membership of UY Per in the clusters is also doubtful (see Walker 1987, and references therein). The eight remaining clusters are listed in Table 1 with their 10 Cepheid variables. We denoted anonymous van den Bergh (C0634+031; van den Bergh 1957) as VDB 1 for brevity. Most of them are close enough that Two Micron All Sky Survey (2MASS) (Skrutskie et al. 2006) photometry reaches well down the MS.

It is likely that all Cepheids in Table 1 are members of their associated clusters. For the three Cepheids in NGC 7790 there exist no radial velocity or proper-motion measurements, although all of them lie near the optical center of the cluster (Sandage 1958). V Cen is located about 25′ away from the center of NGC 5662, but Baumgardt et al. (2000) derived a high membership probability from *Hipparcos* proper motions. The rest of the Cepheids are generally considered to be members of their clusters since they are located within the optical radius defined by bright early-type MS stars and red giants. In many cases, membership is also supported by radial velocities (Mermilliod et al. 1987, and references therein) and proper motions (Baumgardt et al. 2000, and references therein). Orsatti et al. (2001) suggested that TW Nor may not be a member of Lynga 6 from polarization measurements, but we nevertheless included it here.

Previous studies have neglected the effects of cluster metallicity and age on MS fitting (e.g., Feast & Walker 1987; Hoyle et al. 2003). However, the luminosity of the MS at a fixed color (or $T_{\rm eff}$) is sensitive to the metal abundance by $\Delta(m-M)_0/\Delta[{\rm M/H}] \sim 1$ (Paper III). In addition, the cluster age changes the mean color of the upper MS by $\Delta(B-V) \sim 0.05$ between zero-age MS (ZAMS) and ~ 100 Myr isochrone, which is more appropriate for Cepheid-bearing clusters (see below). This, in turn, could affect the reddening estimates from the upper MS by $\Delta E(B-V) \sim 0.05$ and an MS-fitting distance by $\Delta(m-M) \sim 0.1$.

We adopted Cepheid metal abundances from the high-resolution spectroscopy of Fry & Carney (1997) and assumed the same metallicities for the clusters. In support of this assumption, Fry & Carney derived metallicities for two dwarfs in M25 that are in agreement with the metallicity of U Sgr. In addition, Fry & Carney measured $\langle[{\rm Fe/H}]\rangle = +0.01 \pm 0.02$ for two Pleiades dwarfs, which is in good agreement with our adopted value for the Pleiades, $[{\rm Fe/H}] = +0.04 \pm 0.02$.

Fry & Carney also derived α-element abundances (Si, Ca, and Ti) for their sample. For the stars in this paper, the average enhancement is $\langle[\alpha/{\rm Fe}]\rangle = 0.14 \pm 0.02$. We determined an effective metallicity [M/H] from the measured [Fe/H] and [α/Fe] using the Kim et al. (2002) procedure. These abundances are shown in the fourth column of Table 1. The mean metal abundance of our sample is $\langle[{\rm M/H}]\rangle = +0.03 \pm 0.03$ and the standard deviation is 0.08 dex, indicating an intrinsic spread in metallicity for our clusters. On average, the rescaled [M/H] are larger than [Fe/H] by 0.06 dex. We computed errors in [M/H] by propagation of errors in [Fe/H] and [α/Fe].

The metallicity scale for the Cepheids is probably robust to ~ 0.1 dex. As part of a larger study, Yong et al. (2006) reanalyzed spectra of 11 Cepheids in Fry & Carney and derived lower [Fe/H] by ≈ 0.1 dex and lower α-element enhancement by ≈ 0.05 dex on average. The mean difference in the total metallicity is $\Delta\langle[{\rm M/H}]\rangle = -0.15 \pm 0.03$, in the sense that the new analysis indicates lower values. Independently, Andrievsky et al. (2002) measured abundances of 19 Cepheids in common with Fry & Carney. The average difference between these two studies is ≈ 0.1 dex in [Fe/H], the Andrievsky et al. values being larger. They also showed that the alpha abundance ratio ([Si, Ca, Ti/Fe]) is nearly solar, which results in a small difference in the total metal abundance between Fry & Carney and Andrievsky et al., $\Delta\langle[{\rm M/H}]\rangle = -0.01 \pm 0.02$.

We adopted a single representative age (80 Myr) for all clusters, based on comparing our isochrones (§ 3.1) to the cluster CMDs (§ 2.2), and took its uncertainty as $\Delta \log t({\rm Myr}) = 0.2$ ($t = 80^{+50}_{-30}$ Myr). The uncertainty represents both a range of ages among the clusters and the accuracy of the fitting. The average age in the Lynga Open Clusters Catalog (Lynga 1987) is 72 Myr for our sample clusters with a standard deviation of 38 Myr. Previous age estimates based on isochrone fitting are generally within our adopted age range. Mermilliod (1981) found that NGC 7790 and NGC 6067 are about as old as the Pleiades (78 Myr) from models with core overshooting. Meynet et al. (1993) estimated ≈ 70 Myr for NGC 5662 and NGC 6087 when the Pleiades is 100 Myr old from core-overshooting models, while the age of NGC 6067

TABLE 1
LIST OF CEPHEID CLUSTERS AND CEPHEID PROPERTIES

Cluster	Other Name[a]	Cepheid	[M/H][b]	log P	$\langle B\rangle$	$\langle V\rangle$	$\langle I_C\rangle$	$\langle J\rangle$	$\langle H\rangle$	$\langle K_s\rangle$
NGC 129	C0027+599	DL Cas	$+0.08\pm0.03$	0.903	10.119	8.969	7.655	···	···	···
VDB 1[c]	C0634+031	CV Mon	$+0.07\pm0.08$	0.731	11.607	10.304	8.646	7.310	6.783	6.475
NGC 5662	C1431–563	V Cen	$+0.00\pm0.03$	0.740	7.694	6.820	5.805	5.006	4.623	4.462
Lynga 6	C1601–517	TW Nor	$+0.12\pm0.05$	1.033	13.672	11.667	9.287	7.403	6.686	6.225
NGC 6067	C1609–540	V340 Nor	-0.14 ± 0.05	1.053	9.526	8.370	7.168	6.192	5.724	5.515
NGC 6087	C1614–577	S Nor	$+0.05\pm0.03$	0.989	7.373	6.429	5.422	4.661	4.269	4.115
M25	C1828–192	U Sgr	$+0.10\pm0.06$	0.829	7.792	6.695	5.448	4.511	4.085	3.892
NGC 7790	C2355+609	CEa Cas	···	0.711	12.070	10.920	9.470[d]	···	···	···
NGC 7790	C2355+609	CEb Cas	···	0.651	12.220	11.050	9.690[d]	···	···	···
NGC 7790	C2355+609	CF Cas	-0.11 ± 0.05	0.688	12.335	11.136	9.754	···	···	···

[a] "C" cluster designation from Lynga (1987).
[b] An effective metallicity estimated from [Fe/H] and [α/Fe] in Fry & Carney (1997) using the Kim et al. (2002) procedure.
[c] Also named CV Mon cluster or anonymous VDB cluster (van den Bergh 1957).
[d] Taken from Tammann et al. (2003).

was estimated to be ≈ 170 Myr. Cluster ages can also be inferred from the masses of Cepheids. There are several classical Cepheids in binary systems, and these have dynamical masses of about $5-6M_\odot$ (Böhm-Vitense et al. 1998; Evans & Bolton 1990; Evans et al. 1997, 1998, 2006) over the period range similar to those of our sample [$0.65 \leq \log P(\mathrm{days}) \leq 1.05$]. For our models, stars of this mass range have an MS lifetime of about $50-80$ Myr.

2.2. *Photometry*

For the photometry of the Cepheids, we used intensity-mean apparent magnitudes in BVI_C from Berdnikov et al. (2000), which are on the Cape (Cousins) system as realized by Landolt (1983, 1992). For CEa Cas and CEb Cas, the I_C-band measurements were taken from Tammann et al. (2003). We adopted *JHK* photometry from Laney & Stobie (1992) on the Carter (1990) system and transformed it to the LCO system using the Persson et al. (2004) transformation equations. We assumed 0.025 mag zero-point error in the Cepheid photometry and treated this error independently from the cluster photometry (see below). Table 1 lists the Cepheid photometry.

For the cluster photometry, we compiled photoelectric and CCD BVI_C data on the Johnson-Cousins system from the literature, as well as from WEBDA (Mermilliod & Paunzen 2003).[1] The references for the photometry are shown in Table 2, where we used WEBDA's cross-identification of optical sources among different references except for a few cases where we found missing entries and misidentifications. For each cluster we picked one or two references to define a local standard in V or $B-V$ by weighing factors such as the number of observations, number of stars with photometry, magnitude range in V, the photometric calibration procedure, and whether the photometry was generally in agreement with data in other studies. The remaining columns of Table 2 show the mean differences in V and $B-V$ with respect to the local standard, and the number of stars in common. The errors shown are standard errors of the mean difference. For VDB 1 we combined the photoelectric photometry by Arp (1960) and CCD photometry by Turner et al. (1998, their Table 2), whose photometry was tied to the former study.

In most cases the differences between one study and another showed no trends with magnitude. In M25, however, the differences in $B-V$ between Johnson (1960) and Sandage (1960) were statistically significant ($> 2.5\sigma$):

$$\Delta(B-V)(\mathrm{Sandage}-\mathrm{Johnson}) = +0.009(V-10)-0.010.$$

Similarly, in NGC 6087 there were significant trends with magnitude for Fernie (1961) and Breger (1966) with respect to Turner (1986):

$$\Delta V(\mathrm{Fernie}-\mathrm{Turner}) = -0.033(V-10)-0.052,$$
$$\Delta V(\mathrm{Breger}-\mathrm{Turner}) = -0.014(V-10)+0.002.$$

We applied these corrections to put them on the same scale as the reference photometry. For NGC 7790 we only used the photometry by Stetson (2000), although we computed the differences with respect to other studies and included these in Table 2. We applied zero-point corrections to individual values if the average difference was significant at the 2.5σ level. After shifting to a common scale, magnitudes and colors in multiple studies were averaged together. The weighted rms differences between the studies in Table 2 are 0.026 mag in V and 0.024 mag in $B-V$. We therefore adopted 0.025 mag as the characteristic size of systematic errors in the photometry.

Useful $V-I_C$ photometry for MS fitting is limited only to four clusters: VDB 1 (Turner et al. 1998), Lynga 6 (Walker 1985), NGC 6067 (Piatti et al. 1998), and NGC 7790 (Romeo et al. 1989; Gupta et al. 2000; Stetson 2000). As with $B-V$ we adopted the Stetson (2000) photometry for NGC 7790. Compared to Stetson's data, the photometry in Romeo et al. (1989) is bluer by 0.026 ± 0.003 mag, and the photometry in Gupta et al. (2000) is redder by 0.023 ± 0.001. Assuming these values as a characteristic size of error, we adopted 0.025 mag for the photometric zero-point error in $V-I_C$.

We combined optical photometry with JHK_s measurements from the All Sky Data Release of the 2MASS Point Source Catalog (PSC)[2]. WEBDA provides celestial coordinates for only a small fraction of stars in this study. For the others we identified each source on the images from the Digitized Sky Survey,[3] or we computed the celestial coordinates from

[1] See http://obswww.unige.ch/webda/webda.html.

[2] See http://www.ipac.caltech.edu/2mass/.

[3] The Digitized Sky Surveys were produced at the Space Telescope Science Institute under US Government grant NAG W-2166. The images of these surveys are based on photographic data obtained using the Oschin Schmidt Telescope on Palomar Mountain and the UK Schmidt Telescope. The plates were processed into the present compressed digital form with the permission of these institutions.

TABLE 2
PHOTOMETRY REFERENCES AND ZERO-POINT DIFFERENCES

Reference	ΔV	$N_{\rm comp}$	$\Delta(B-V)$	$N_{\rm comp}$
		NGC 129		
Arp et al. (1959)	$+0.010 \pm 0.006$	26	$+0.004 \pm 0.011$	26
Hoag et al. (1961)	$+0.000 \pm 0.011$	18	$+0.059 \pm 0.008$	18
Turner et al. (1992)	$+0.015 \pm 0.006$	20	$+0.048 \pm 0.008$	22
Phelps & Janes (1994)	standard	···	standard	···
		VDB 1		
Arp (1960)	standard	···	standard	···
Turner et al. (1998)	tied to Arp	···	tied to Arp	···
		NGC 5662		
Moffat & Vogt (1973)	$+0.009 \pm 0.005$	13	$+0.002 \pm 0.004$	28
Haug (1978)	standard	···	$+0.027 \pm 0.004$	20
Clariá et al. (1991)	$+0.051 \pm 0.004$	19	standard	···
Sagar & Cannon (1997)	-0.021 ± 0.015	10	$+0.004 \pm 0.006$	14
		Lynga 6		
Madore (1975)	$+0.009 \pm 0.015$	8	-0.002 ± 0.010	9
Moffat & Vogt (1975)	-0.097 ± 0.018	9	-0.030 ± 0.025	10
van den Bergh & Harris (1976)	-0.010 ± 0.008	12	$+0.024 \pm 0.014$	12
Walker (1985)	standard	···	standard	···
		NGC 6067		
Thackeray et al. (1962)	-0.019 ± 0.013	15	$+0.012 \pm 0.008$	14
Walker & Coulson (1985)	standard	···	standard	···
Piatti et al. (1998)	-0.021 ± 0.003[a]	123	···	···
		NGC 6087		
Fernie (1961)	-0.057 ± 0.020	9	$+0.041 \pm 0.006$	10
Breger (1966)	$+0.005 \pm 0.008$	18	-0.019 ± 0.011	17
Turner (1986)	standard	···	standard	···
Sagar & Cannon (1997)	$+0.080 \pm 0.070$	2	$+0.025 \pm 0.035$	2
		M25		
Johnson (1960)	-0.018 ± 0.003	74	standard	···
Sandage (1960)	$+0.018 \pm 0.005$	51	$+0.005 \pm 0.004$	68
Wampler et al. (1961)	standard	···	$+0.021 \pm 0.004$	51
		NGC 7790		
Sandage (1958)	-0.010 ± 0.013	26	-0.018 ± 0.008	26
Romeo et al. (1989)	-0.001 ± 0.003	186	$+0.013 \pm 0.003$	184
Phelps & Janes (1994)	-0.030 ± 0.001	360	-0.005 ± 0.002	337
Lee & Lee (1999)	$+0.027 \pm 0.003$	164	-0.032 ± 0.003	157
Gupta et al. (2000)	$+0.008 \pm 0.001$	192	$+0.009 \pm 0.002$	187
Stetson (2000)	standard	···	standard	···

NOTE. — The mean color and magnitude differences are computed after 3σ rejection. Uncertainties are the standard error of the mean. The differences are in the sense of individual values minus those adopted as the local standard. The photometry in Turner et al. (1998) are directly tied to the photometry of Arp (1960).

[a]Comparison for stars with $V \leq 15$.

the plate position information in WEBDA. The rms difference between the retrieved and the 2MASS coordinates was typically $0.5''$. For NGC 6067 we matched 2MASS sources with optical photometry only for those stars with good positional accuracy. The validation of the 2MASS source matches was confirmed from the resulting tight optical and near-infrared color-color relations. Based on PSC flag parameters, we ignored the infrared data if sources were undetected, blended, or contaminated. Calibration errors in JHK_s were taken as the uncertainty specified in the explanatory supplement to the 2MASS All Sky Data Release: 0.011 mag in J, 0.007 mag in H, and 0.007 mag in K_s.[4]

Most studies do not report individual errors in optical magnitude or color, so we computed the median of V and $B-V$ differences from various studies (after shifting to a common scale using the $> 2.5\sigma$ criterion) and assigned this value to represent the random photometric errors for all stars in each cluster. For $V-I_C$ we assigned 0.02 mag as the random error. Errors for individual stars in Stetson (2000) were adopted without change. The $V-K_s$ errors were computed as the quadrature sum of V errors and the catalog's "total" photometric uncertainties in K_s.

The cluster CMDs in various color combinations are shown in Figures 1 through 4. Stars rejected as being far from the MS are shown as open circles, while those used in the MS fitting are shown as bull's-eyes. The curved line in each panel is the best-fitting isochrone on each CMD. Details of the MS fitting and outlier rejection are given in the next section. Throughout this paper we denote CMDs by their color and luminosity indices as $(B-V,V)$, $(V-I_C,V)$, $(V-K_s,V)$, $(J-K_s,K_s)$, and $(H-K_s,K_s)$.

3. MAIN-SEQUENCE FITTING

3.1. *Extension of Isochrone Calibration*

In our first two papers of this series (Paper I and Paper II), we assessed the accuracy of distances from MS fitting and examined systematic errors in the transformation of theoretical to observational quantities. In Paper I we demonstrated that stellar models from the Yale Rotating Evolutionary Code

[4] See http://www.ipac.caltech.edu/2mass/releases/allsky/doc/explsup.html.

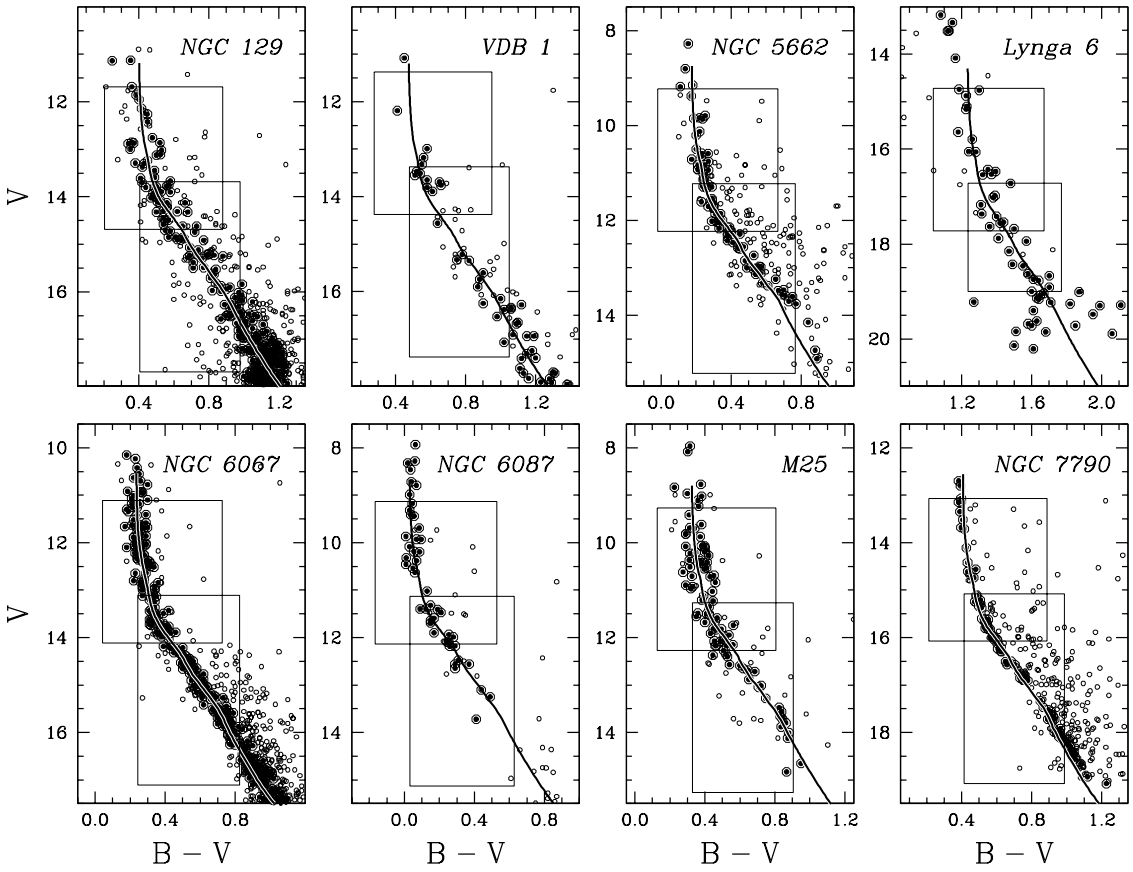


FIG. 1.— Cluster CMDs in $B-V$. The bull's-eyes are stars remaining after the photometric filtering, while open circles are stars rejected. The solid lines are empirically calibrated isochrones at the best-fitting distance (Tables 6), reddening (Tables 7), and $R_{V,0}$ (Tables 9). The boxes on the upper MS and lower MS are regions where the color excess and distance were determined, respectively.

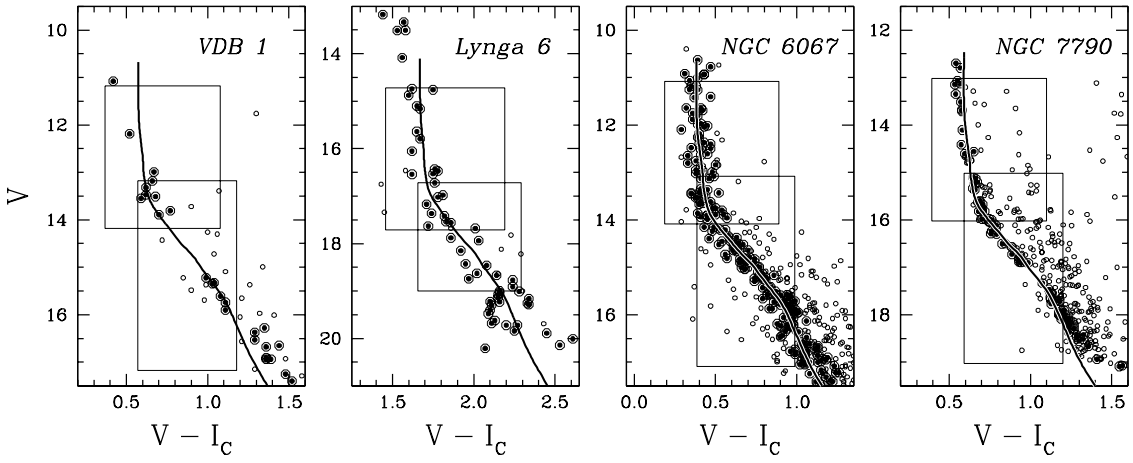


FIG. 2.— Same as Fig. 1, but CMDs in $V-I_C$.

(Sills et al. 2000) are in agreement with the masses and luminosities of the well-studied Hyades eclipsing binary vB 22 (Torres & Ribas 2002). These models also satisfy stringent tests from helioseismology and predict solar neutrino fluxes in line with observations (Basu et al. 2000; Bahcall et al. 2001; Bahcall & Pinsonneault 2004). In Paper II we showed that the models provide a good match to the spectroscopically determined temperatures (Paulson et al. 2003) of individual Hyades members with good parallaxes (de Bruijne et al. 2001). However, we found that any of the widely-used color-$T_{\rm eff}$ relations (e.g., Alonso et al. 1995, 1996; Lejeune et al. 1997, 1998, hereafter LCB) fail to reproduce the observed shapes of the MS in the Hyades, having differences in broad-band colors as large as 0.1 mag. The existence of these systematic errors in the colors, in the presence of agreement between the spectroscopic and theoretical luminosity-$T_{\rm eff}$ scales, led us to argue that the problems lie with the adopted color-$T_{\rm eff}$ relations instead of errors in the theoretical $T_{\rm eff}$ scale. We

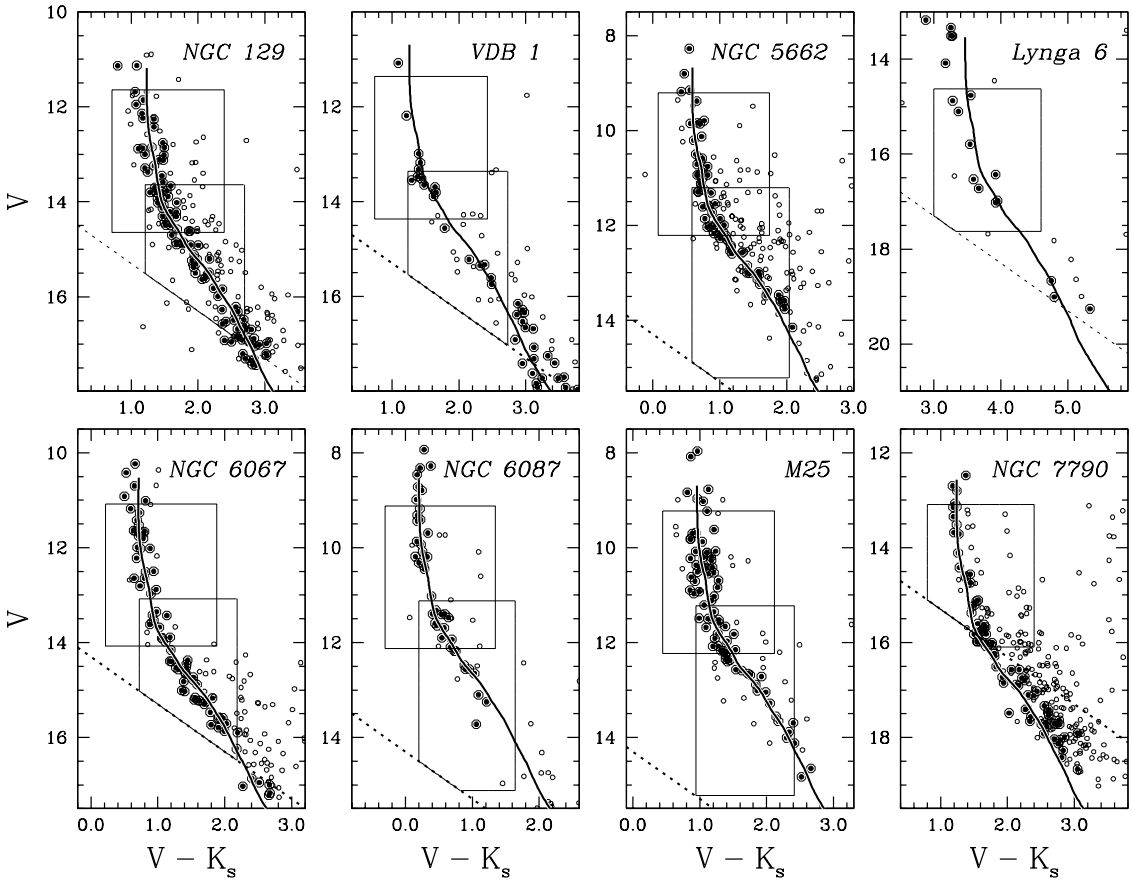


FIG. 3.— Same as Fig. 1, but CMDs in $V-K_s$. The dotted line represents the 2MASS completeness limit.

then adopted the LCB color-$T_{\rm eff}$ relations and computed empirical corrections to the LCB relations to match photometry in the Hyades. In Paper III we showed that isochrones with the empirical color-$T_{\rm eff}$ corrections accurately match the MS shapes of other nearby clusters in three color indices ($B-V$, $V-I_C$, and $V-K_s$), yielding distance estimates with errors as small as 0.04 mag in distance modulus (or 2% in distance).

However, the Hyades-based calibration is of limited use for this study. The calibration is reliable only at $M_V \gtrsim 3$ because the number of stars in the upper MS of the Hyades is small in this relatively old open cluster (550 Myr from models excluding convective overshoot; Perryman et al. 1998). On the other hand, photometry of our sample clusters is quite sparse or absent in this lower MS part. It is therefore desirable to define an extension of the empirical color-$T_{\rm eff}$ corrections for hotter and brighter stars. A good choice for a calibrating cluster is the Pleiades for several reasons. First of all, its geometric distance is now known to a precision comparable to that of the Hyades, $(m-M)_0 = 5.63 \pm 0.02$ (see Paper III and references therein for a detailed discussion of the cluster parameters). Second, it has low reddening, $E(B-V) = 0.032 \pm 0.003$. Third, a precise metal abundance from high-resolution spectra is available, [Fe/H] = $+0.04 \pm 0.02$. Furthermore, Cepheid clusters tend to be of ages comparable to that of the Pleiades, making it a good template for distance and reddening estimates.

The sources of our Pleiades photometry are described in Paper III. We began by removing a few known binaries and then rejected stars that are more than 0.1 mag in color away from a 15 point median of the sample sorted in V; this step was independent of the theoretical isochrones. Table 3 lists photometry of the hot Pleiades stars that remained after this selection. The CMDs of these stars are shown in Figure 5. Small plus signs denote stars rejected as far from the MS, while open circles show stars retained for use in the following calibration process.

In the course of this work we became aware of some problematic features in the LCB color tables. They computed synthetic colors from both the "original" and the "corrected" model flux distributions (hereafter original and corrected LCB tables, respectively). In Figure 6 we compare the corrected LCB table with the original LCB table for MS stars ($\log g$ = 4.5). The LCB empirical color-$T_{\rm eff}$ relations (corrected LCB table) are defined only for $T_{\rm eff} < 11500\,K$, which results in an artificial jump in CMDs, particularly in the V-band bolometric correction. In addition, there are small scale structures in the color corrections (especially in $V-I_C$) that cause interpolation noise in our isochrones at $T_{\rm eff} \gtrsim 8000$ K. We therefore used the original LCB table above 8000 K, the corrected LCB table below 6500 K, and a linear ramp between the two tables in order to produce smoother base isochrones. Isochrones at an age of 100 Myr generated with these "merged" color-$T_{\rm eff}$ relations are shown as dot-dashed lines in Figure 5. However, these still fail to match the observed MS of the Pleiades and therefore require further corrections.

We derived empirical corrections to the isochrone in $B-V$, $V-I_C$, $V-K_s$, and $J-K_s$ by forcing a match to the Pleiades photometry as done for the Hyades (Paper II). Figure 7 plots the difference in color between individual stars and an isochrone generated with the merged LCB color-$T_{\rm eff}$ relations.

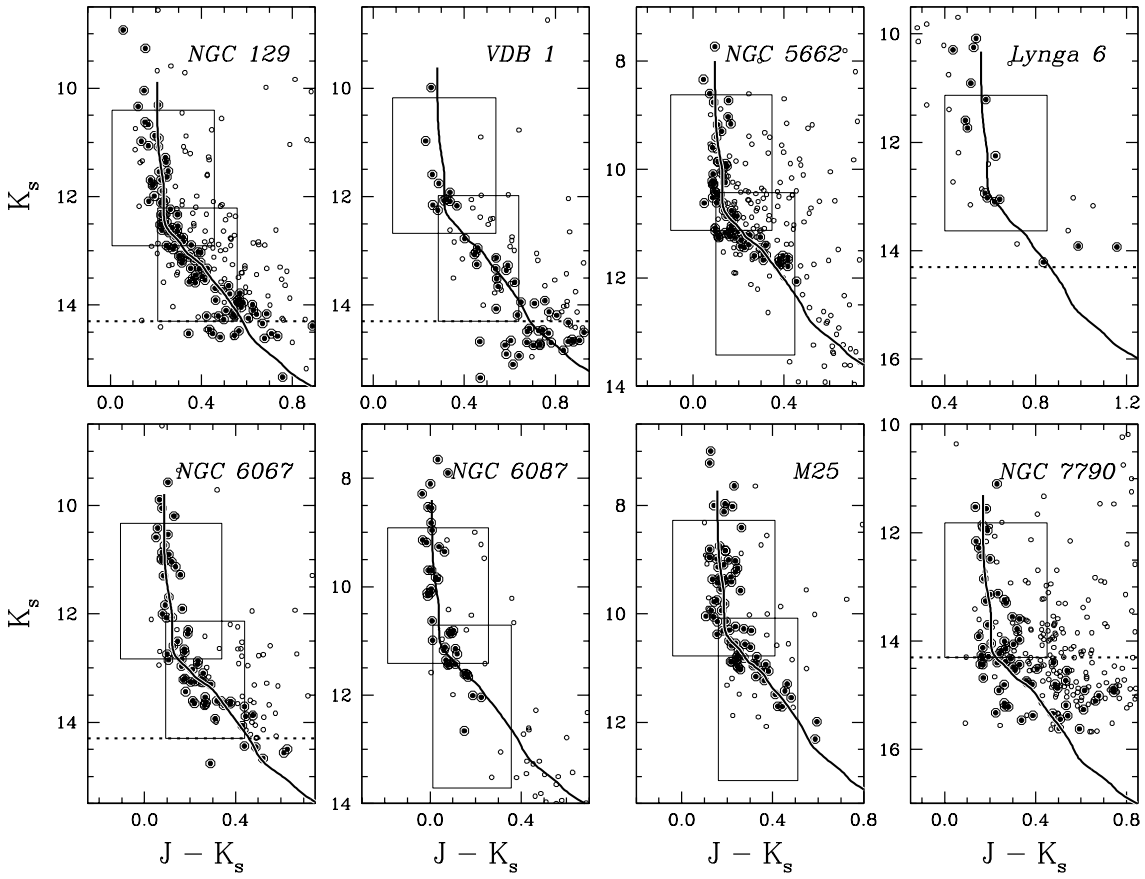


FIG. 4.— Same as Fig. 1, but CMDs in $J-K_s$. The dotted line represents the 2MASS completeness limit.

The $T_{\rm eff}$ was calculated from M_V. Filled circles are for the Pleiades stars, and the open circles are for the Hyades stars used in the calibration of the lower MS. The Pleiades stars have smaller error bars than the Hyades points because we assumed a negligible distance spread for the Pleiades, while the Hyades ones reflect parallax errors for individual stars (de Bruijne et al. 2001). The solid lines in Figure 7 represent our empirical corrections, which were computed at a constant M_V in a seven-point moving window. Given the modest sample size and intrinsic scatter in the upper MS, we did not attempt to resolve out smaller scale structures. We defined the empirical color-$T_{\rm eff}$ corrections as those for the Pleiades at $T_{\rm eff} \geq 6838$ K and for the Hyades at $T_{\rm eff} \leq 6500$ K. A spline function was used to bridge over the narrow $T_{\rm eff}$ gap between these two corrections. We also used $H-K_s$ in MS fitting but without color corrections because photometric errors were too large in this color to provide a reliable calibration.

Applying these corrections to the colors at each $T_{\rm eff}$ defines the empirically calibrated isochrone for the Pleiades, which is tabulated along with the color corrections in Table 4. Isochrones incorporating the corrections for the Pleiades are shown as solid lines in Figure 5. Systematic errors in the color corrections are ~ 0.01 mag from the errors in the adopted distance, metallicity, and reddening values for the Pleiades. We assumed that our empirical corrections in the upper MS are independent of metallicity and age and applied them to all isochrones generated in Paper III. The isochrones constructed in this way are available online at
`http://www.astronomy.ohio-state.edu/iso/`.

There is one important functional difference between the calibration for luminous stars and that for the lower MS stars. The MS for FGK-type stars is intrinsically very narrow. As a result, for the low-mass stars we could plausibly claim that the empirical cluster sequence could be used to redefine the color-$T_{\rm eff}$ relationship. On the other hand, the dispersion about the mean trend for upper MS stars is significantly larger. For the Pleiades, we found a dispersion of 0.02 mag in $B-V$ for $0.0 \lesssim B-V \lesssim 0.40$ (after excluding outliers), which is significantly above the photometric precision. A comparable increase was seen in $V-I_C$ and $V-K_s$ (0.02 and 0.04 mag, respectively). Although this could be due to differential reddening across the cluster field (Breger 1986), the persistence of rapid rotation in early-type stars can impact both their evolution and the mapping of $T_{\rm eff}$ onto colors (e.g., Collins & Sonneborn 1977) as a consequence of the Kraft (1965) break in rotational properties. Furthermore, these effects depend on both the rotation rate and the inclination to the line of sight and can be as large as 0.1 mag in $B-V$. Nonetheless, the mean cluster locus can still be used to define a template for distance studies but should not be interpreted as a direct change in the color-$T_{\rm eff}$ relationship. In other words, our empirical corrections remove systematic trends from the rotation-induced color anomalies, as well as from any intrinsic problems in the adopted color-$T_{\rm eff}$ relationship.

3.2. *Main-Sequence Fitting*

We determined the distance, reddening, and the ratio of total to selective extinction in V [$R_V \equiv A_V/E(B-V)$] for each cluster via an iterative approach, which fits an isochrone to individual CMDs of various color indices. All of these pa-

TABLE 3
MERGED PHOTOMETRY IN THE PLEIADES

ID[a]	M_V	$(B-V)_0$	$(V-I_C)_0$	M_{K_s}	$(V-K_s)_0$	$(J-K_s)_0$	$(H-K_s)_0$
Hz II 153	1.782	0.119	0.134	1.525 ± 0.021	0.257 ± 0.025	0.021 ± 0.025	0.067 ± 0.061
Hz II 447	–0.278	–0.076	–0.029	-0.147 ± 0.008	-0.131 ± 0.016	-0.067 ± 0.022	-0.026 ± 0.036
Hz II 531	2.845	0.306	0.375	2.095 ± 0.019	0.750 ± 0.024	0.136 ± 0.024	0.023 ± 0.035
Hz II 817	0.028	–0.066	–0.013	0.134 ± 0.011	-0.106 ± 0.018	-0.041 ± 0.025	0.043 ± 0.046
Hz II 859	0.692	–0.052	–0.021	0.790 ± 0.019	-0.098 ± 0.024	-0.052 ± 0.027	0.045 ± 0.043
Hz II 1028	1.635	0.069	0.099	1.482 ± 0.019	0.153 ± 0.024	-0.024 ± 0.020	-0.020 ± 0.021
Hz II 1139	3.643	0.450	0.490	2.600 ± 0.019	1.043 ± 0.024	0.212 ± 0.027	0.031 ± 0.022
Hz II 1234	1.087	–0.012	0.033	1.049 ± 0.019	0.038 ± 0.024	-0.011 ± 0.030	0.035 ± 0.060
Hz II 1362	2.528	0.230	0.274	1.996 ± 0.013	0.532 ± 0.019	0.110 ± 0.026	-0.018 ± 0.037
Hz II 1375	0.572	–0.011	–0.006	0.614 ± 0.016	-0.042 ± 0.021	-0.047 ± 0.017	-0.015 ± 0.029
Hz II 1407	2.393	0.220	0.259	1.877 ± 0.016	0.516 ± 0.021	0.080 ± 0.020	0.017 ± 0.019
Hz II 1823	–0.286	–0.102	–0.043	-0.083 ± 0.010	-0.203 ± 0.017	-0.075 ± 0.025	0.024 ± 0.027
Hz II 1993	2.645	0.242	0.313	1.989 ± 0.010	0.656 ± 0.017	0.109 ± 0.019	0.063 ± 0.017
Hz II 2195	2.387	0.190	0.220	1.933 ± 0.011	0.454 ± 0.018	0.079 ± 0.019	0.017 ± 0.029
Hz II 2345	3.375	0.407	0.466	2.393 ± 0.017	0.982 ± 0.022	0.204 ± 0.021	0.055 ± 0.025
Hz II 2717	1.682	0.101	...	...	...	...	...
Hz II 3031	3.105	0.352	0.433	2.234 ± 0.017	0.871 ± 0.022	0.164 ± 0.023	0.047 ± 0.019
Hz II 3302	3.153	0.330	0.381	2.314 ± 0.017	0.839 ± 0.022	0.135 ± 0.024	0.057 ± 0.017
Hz II 3308	3.068	0.320	0.358	2.268 ± 0.011	0.800 ± 0.018	0.157 ± 0.031	0.019 ± 0.046
Hz II 3309	3.438	0.410	0.466	2.451 ± 0.000	0.987 ± 0.014	0.167 ± 0.013	0.078 ± 0.013
Hz II 3310	3.398	0.430	0.498	2.359 ± 0.025	1.039 ± 0.029	0.216 ± 0.027	0.025 ± 0.030
Hz II 3319	2.983	0.330	0.381	2.168 ± 0.008	0.815 ± 0.016	0.137 ± 0.017	0.078 ± 0.011
Hz II 3332	3.338	0.400	0.482	2.343 ± 0.021	0.995 ± 0.025	0.157 ± 0.027	0.014 ± 0.030
Hz II 3334	2.605	0.232	0.306	2.035 ± 0.023	0.570 ± 0.027	0.072 ± 0.027	0.032 ± 0.034
Hz II 5016	2.017	0.149	0.181	1.667 ± 0.021	0.350 ± 0.025	0.061 ± 0.022	0.011 ± 0.025
Hz II 5023	1.282	–0.001	0.010	1.239 ± 0.017	0.043 ± 0.022	-0.046 ± 0.019	0.030 ± 0.023
Hz II 5025	0.337	–0.041	0.018	0.333 ± 0.016	0.004 ± 0.021	-0.027 ± 0.017	0.069 ± 0.061
TS 23	1.002	–0.031	–0.006	1.029 ± 0.016	-0.027 ± 0.021	-0.049 ± 0.024	-0.003 ± 0.017
TS 25	1.377	0.009	0.010	1.389 ± 0.013	-0.012 ± 0.019	-0.071 ± 0.021	-0.013 ± 0.037
TS 78	2.092	0.159	0.173	1.724 ± 0.025	0.368 ± 0.029	0.051 ± 0.031	0.023 ± 0.033
TS 84	2.272	0.190	0.228	1.894 ± 0.010	0.378 ± 0.017	0.049 ± 0.016	0.044 ± 0.052
TS 115	2.583	0.230	0.259	2.063 ± 0.019	0.520 ± 0.024	0.080 ± 0.021	0.041 ± 0.027
TS 137	2.002	0.149	0.181	1.596 ± 0.019	0.406 ± 0.024	0.055 ± 0.028	0.022 ± 0.033
TS 165	1.907	0.129	0.095	1.641 ± 0.010	0.266 ± 0.017	0.007 ± 0.013	0.042 ± 0.011
TS 194	1.462	0.009	0.010	1.474 ± 0.016	-0.012 ± 0.021	-0.032 ± 0.017	-0.038 ± 0.026

[a]The star designation is that of Hertzsprung (1947), Hz II; and Trumpler (1921), TS.

TABLE 4
EMPIRICALLY CALIBRATED PLEIADES ISOCHRONE

$T_{\rm eff}$ (K)	$M_{V,0}$	$(B-V)_0$	$(V-I_C)_0$	$(V-K_s)_0$	$(J-K_s)_0$	$\Delta(B-V)$	$\Delta(V-I_C)$	$\Delta(V-K_s)$	$\Delta(J-K_s)$
12484	–0.034	–0.073	–0.023	–0.128	–0.056	0.041	0.084	0.155	0.030
12286	0.100	–0.068	–0.020	–0.115	–0.053	0.041	0.083	0.154	0.029
11769	0.414	–0.053	–0.012	–0.079	–0.046	0.044	0.083	0.156	0.028
11153	0.723	–0.040	–0.008	–0.052	–0.045	0.038	0.073	0.130	0.017
10468	1.053	–0.017	0.005	–0.012	–0.044	0.032	0.066	0.102	0.001
9881	1.335	0.016	0.026	0.034	–0.039	0.030	0.059	0.074	–0.011
9404	1.569	0.056	0.060	0.112	–0.021	0.033	0.063	0.080	–0.009
9020	1.769	0.097	0.101	0.200	0.002	0.039	0.070	0.096	–0.001
8684	1.956	0.134	0.142	0.285	0.024	0.036	0.071	0.103	0.006
8383	2.138	0.166	0.183	0.358	0.044	0.028	0.063	0.084	0.008
8107	2.316	0.194	0.224	0.433	0.063	0.006	0.042	0.049	0.005
7853	2.487	0.221	0.269	0.527	0.084	–0.006	0.030	0.037	0.002
7606	2.652	0.254	0.313	0.629	0.103	–0.014	0.025	0.032	–0.004
7362	2.819	0.290	0.349	0.724	0.123	–0.016	0.021	0.034	–0.007
7128	2.993	0.324	0.384	0.807	0.141	–0.017	0.016	0.032	–0.008
6932	3.167	0.360	0.424	0.882	0.157	–0.014	0.015	0.031	–0.011
6838	3.261	0.380	0.446	0.925	0.167	–0.011	0.015	0.028	–0.013

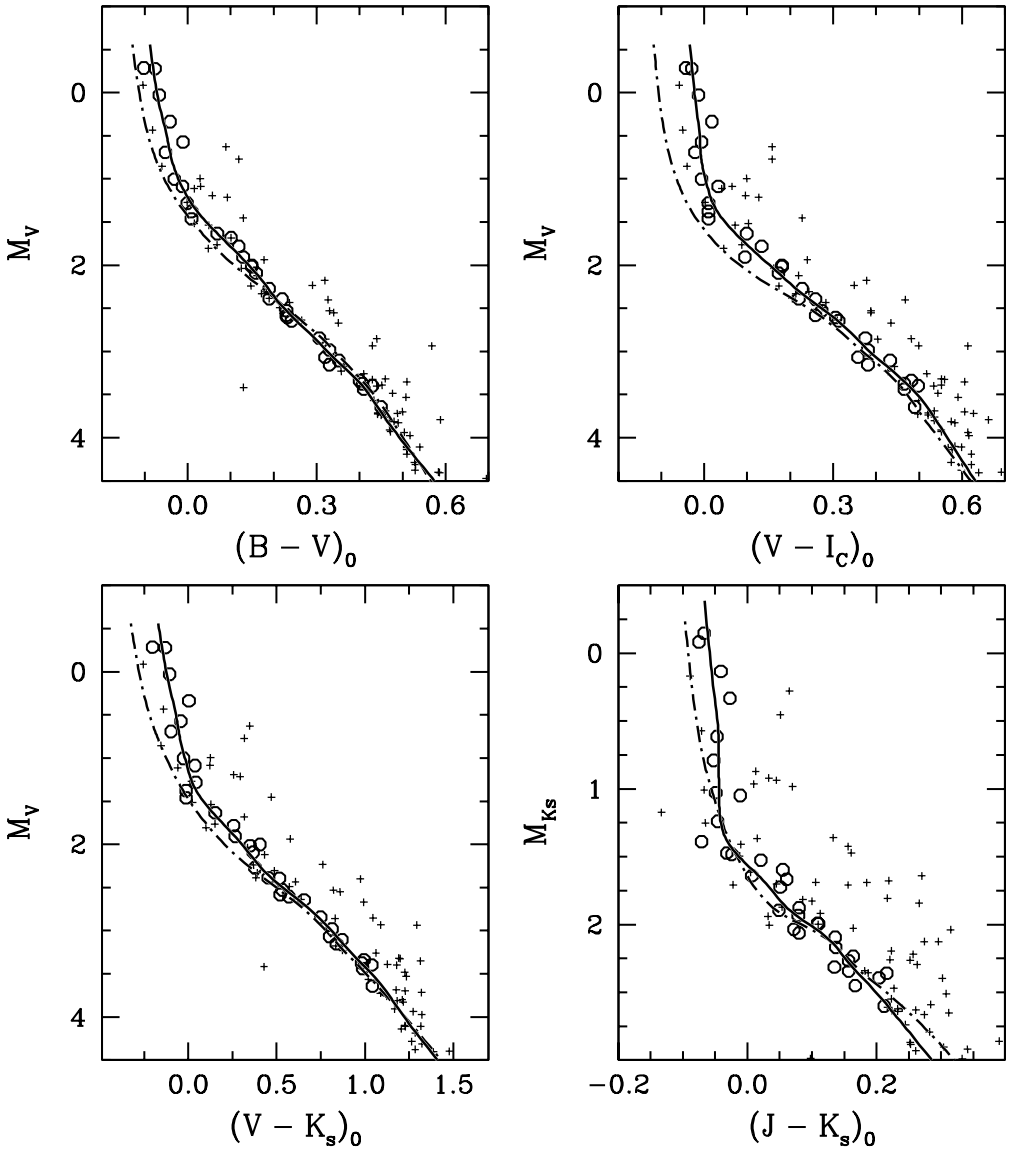


FIG. 5.— Empirically calibrated isochrones for the Pleiades (*solid lines*). The dot-dashed lines show the isochrones without the color corrections. The open circles are stars retained for use in the calibration process, and the small plus signs show stars rejected (see text).

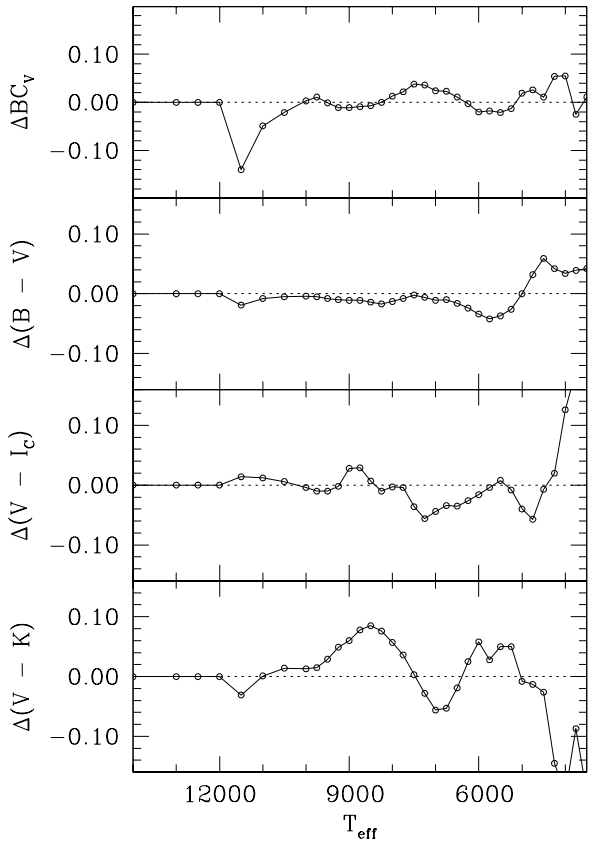


FIG. 6.— Differences in the bolometric correction and colors between "corrected" and "original" LCB tables for MS stars ([M/H] = 0, $\log g$ = 4.5). Differences are in the sense of the former minus the latter values.

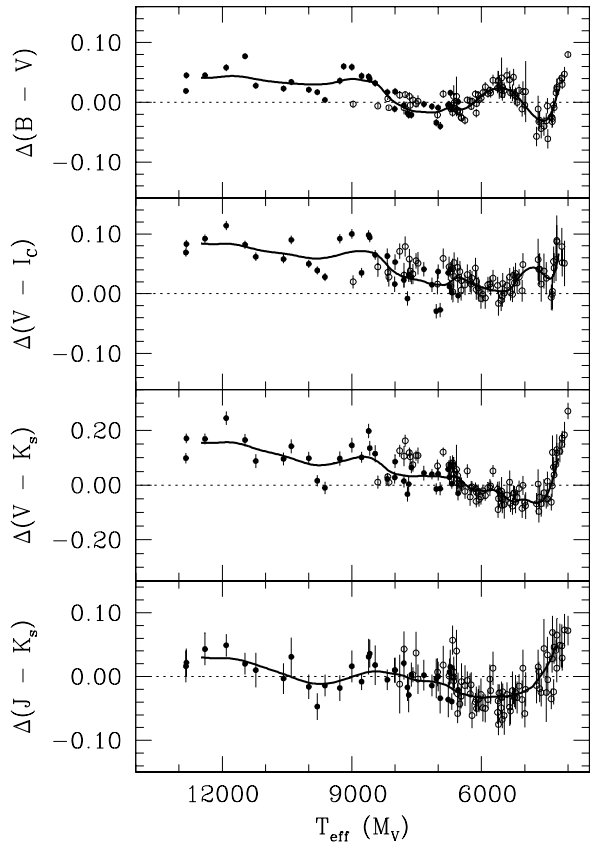


FIG. 7.— Empirical color-$T_{\rm eff}$ corrections (*solid line*). The filled circles show the differences in colors between the Pleiades data and the uncorrected isochrone at a constant M_V. The sense of the difference is the former minus the latter values. The open circles are those for the Hyades stars.

rameters are essential to obtain self-consistent solutions for the absolute magnitude of a Cepheid (§ 5). Our MS-fitting process also includes rejection of stars that are too far away from an MS ridge-line, defined by the locus of points with the highest density on each CMD. Individual color excesses in each cluster were used to derive R_V according to the extinction law described by Cardelli et al. (1989, hereafter CCM89). The rest of this section describes the MS-fitting process in detail.

Our sample clusters do not have detailed radial velocity or proper-motion membership studies. Before isochrone fitting we therefore applied the photometric filtering procedure described in Paper III to identify and reject stars that are likely foreground/background objects or cluster binaries. The procedure iteratively identifies a cluster MS ridge-line independently of the isochrones and rejects stars if they are too far away from the ridge-line. This was done by computing χ^2 in each CMD as

$$\chi^2 = \sum_{i=1}^{N} \chi_i^2 = \sum_{i=1}^{N} \frac{(\Delta X_i)^2}{\sigma_{X,i}^2 + (\gamma_i^{-1}\sigma_{V,i})^2 + \sigma_0^2}, \qquad (1)$$

where ΔX_i is the color difference between the i^{th} data point and MS at the same V; $\sigma_{X,i}$ and $\sigma_{V,i}$ are photometric errors in color and V, respectively. The error in V contributes to the error in ΔX_i by the inverse slope of the MS, γ_i^{-1}. We added σ_0 in quadrature to the propagated photometric errors in the denominator to take into account the presence of differential reddening, cluster binaries, non-cluster members, and other effects that would increase the MS width above the photometric precision. We adjusted the value of σ_0 so that the total χ^2 is equal to the total number of stars N used in the filtering.

Initially we rejected all data points as outliers if χ_i^2 (the individual contribution to χ^2) was greater than 9 (corresponding to a 3σ outlier). We repeated adjusting σ_0 and rejecting outliers with the reduced set of data points until there remained no point with $\chi_i^2 > 9$. We combined the results from all CMDs, and rejected stars if they were tagged as an outlier at least in one of the CMDs. Missing data in any colors was not a criterion for rejection. For this study we included $(J-K_s, K_s)$ and $(H-K_s, K_s)$ in the filtering procedure. We reduced the rejection threshold at each iteration until it was limited to 2.0–2.4σ, but our result is insensitive to the final rejection threshold within the fitting errors.

Our filtering results are shown in Figures 1–4. The bull's-eyes represent stars retained and used in the following MS fits, and open circles are the ones rejected by the filtering. At the end of the iteration, σ_0 values in $(B-V,V)$ and $(V-K_s,V)$ were (0.055 mag, 0.101 mag) in NGC 129, (0.050 mag, 0.102 mag) in VDB 1, (0.023 mag, 0.064 mag) in NGC 5662, (0.048 mag, 0.102 mag) in Lynga 6, (0.031 mag, 0.078 mag) in NGC 6067, (0.033 mag, 0.058 mag) in NGC 6087, (0.043 mag, 0.111 mag) in M25, and (0.011 mag, 0.026 mag) in NGC 7790. These excess dispersions are most likely due to differential reddening of heavily reddened, young open clusters. Note that the ratio of σ_0 values from $(B-V,V)$ and $(V-K_s,V)$ is also approximately equal to the color-excess ratio $E(V-K_s)/E(B-V) \approx 2.8$ (see below). We discuss in detail the effects of differential reddening on *P-L* relations in § 5. In

$(J-K_s,K_s)$ and $(H-K_s,K_s)$, photometric errors were usually large enough that σ_0 values were automatically set to zero.

The fitting process took advantage of the changing slope of the MS with absolute magnitude. Near the MS turnoff ($M_V \leq 1.5$), the MS is nearly vertical, allowing a precise determination of the reddening. Further down ($1.5 \leq M_V \leq 3.5$), the slope of the MS is still relatively steep [e.g., $\Delta M_V/\Delta(B-V) \approx 5$], but it nevertheless provides sufficient leverage for determining the distance. We divided each CMD into two zones, shown as boxes in Figures 1–4, which define the regions used for determining the color excess and distance. The color excess was determined for stars with $-1.0 \leq M_V \leq 2.0$ in $(B-V,V)$, $(V-I_C,V)$, and $(V-K_s,V)$, and at $-0.8 \leq M_K \leq 1.7$ in $(J-K_s,K_s)$ and $(H-K_s,K_s)$. Distance determinations came from stars with $-0.1 \leq (B-V)_0 \leq 0.5$ and the corresponding color ranges in other colors with the same M_V. For Lynga 6 and NGC 7790, $(V-K_s,V)$ and $(J-K_s,K_s)$ were not used in the distance estimation because the lower parts of the MS are below the 2MASS completeness limit ($K_s \approx 14.3$).

Since the color excess and R_V depend on the intrinsic color of stars, we adopted the color-dependent relations from Bessell et al. (1998, hereafter BCP98) and M. S. Bessell (2007, private communication). Their formulae were based on the theoretical stellar spectral energy distributions with the extinction law from Mathis (1990). Specifically, their formulation yields

$$R_V = R_{V,0} + 0.22(B-V)_0, \tag{2}$$

$$E(B-V) = E(B-V)_0\{1-0.083(B-V)_0\}, \tag{3}$$

where $(B-V)_0$ is an intrinsic color of each star. The $R_{V,0}$ and $E(B-V)_0$ are the values for zero-color stars, where $R_{V,0}$ is 3.26 in their model. For other colors we used the following color-excess ratios:

$$\frac{E(V-I_C)}{E(B-V)} = 1.30 + 0.06(V-I_C)_0 \tag{4}$$

$$\frac{E(V-K_s)}{E(B-V)} = 2.88 + 0.07(V-K_s)_0 \tag{5}$$

$$\frac{E(J-K_s)}{E(B-V)} = 0.56 + 0.06(J-K_s)_0 \tag{6}$$

$$\frac{E(H-K_s)}{E(B-V)} = 0.20 + 0.15(H-K_s)_0. \tag{7}$$

The first terms represent the color-excess ratios from CCM89 at $R_{V,0}$ = 3.26, and the second terms are color-dependent relations from BCP98. Differences between the original coefficients in BCP98 and those for the 2MASS JHK_s system using transformation equations in Carpenter (2001)[5] were found to be negligible. Table 5 lists color-excess ratios for zero-color stars from CCM89 and BCP98, as well as observationally derived values from Schultz & Wiemer (1975), Dean et al. (1978), Sneden et al. (1978), and Rieke & Lebofsky (1985). Color-excess ratios determined from our cluster sample are also shown in the fourth column, which is discussed in the next section.

The fitting process begins with a guess at the average distance. At this distance, individual color excesses for zero-color stars [$E(B-V)_0^{\rm obs}$, $E(V-I_C)_0^{\rm obs}$, etc.] were determined using stars on the upper MS. These were used to determine the best-fit $R_{V,0}$ and $E(B-V)_0$ from the CCM89 extinction law by minimizing

$$\chi^2 = \sum_{i=1}^{5}\left[\frac{E(\lambda_i-V)_0^{\rm obs} - E(\lambda_i-V)_0^{\rm CCM89}}{\sigma_{E(\lambda-V)}}\right]^2, \tag{8}$$

where λ_i represents effective wavelengths in BI_C (Bessell et al. 1998) and isophotal wavelengths in JHK_s (Cohen et al. 2003). The index in the summation runs over B, I_C, J, H, and K_s. The $\sigma_{E(\lambda-V)}$ is the fitting error in the upper MS, which was determined from the scatter of the points around the isochrone and the individual errors in color. The CCM89 color excess, $E(\lambda-V)_0^{\rm CCM89}$, can be expressed as

$$E(\lambda-V)_0^{\rm CCM89} = R_{V,0}E(B-V)_0\left(\frac{A_\lambda}{A_V}-1\right), \tag{9}$$

where A_λ/A_V is a function of $R_{V,0}$ from polynomial relations in CCM89. Note that $R_{V,0}$ and $E(B-V)_0$ in equation (8) are two parameters to be determined and that $E(B-V)_0$ in equation (9) is the normalization factor, which is different from the input color excess in $(B-V,V)$.

The fitting procedure then found weighted median distances on each CMD by using the stars in the lower part of the MS. The weighted average distance from all CMDs was computed, and the process was repeated until convergence, which occurred when the difference in the average distance from the previous iteration became smaller than its propagated error.

An example of the fit is shown in Figure 8 for NGC 6067. The solid line in the top panel is the best-fitting CCM89 extinction curve to the data (*open circles*). The bottom panel shows likelihood contours in $R_{V,0}$ and $E(B-V)_0$ drawn at $\Delta\chi^2$ = 2.30, 6.17, and 11.8 from the minimum χ^2 = 4.5 (68.3%, 95.4%, and 99.73% confidence levels for 2 degrees of freedom).

4. CLUSTER PROPERTIES

In this section we present our results on the distance, reddening, and R_V of the sample clusters and evaluate various systematic errors in these parameters. In particular, we assess the accuracy of MS-fitting based on internal consistency of distances from multi-color CMDs. We show that our distance estimates are generally shorter than previous ZAMS-fitting results and that this is mainly due to our lower reddening estimates.

4.1. *Distance, Reddening, and R_V*

Our MS-fitting results on the distance and color excess from individual CMDs are shown in Tables 6 and 7, respectively, along with a number of stars used in the fit. The last two columns in Table 6 show the weighted average distance modulus from all available CMDs with its propagated error and the standard deviation (σ) of individual distances. The last column in Table 7 lists a standard deviation of $E(B-V)$ from all CMDs, after transforming individual color-excess values in $V-I_C$, $V-K_s$, and $J-K_s$ to $E(B-V)$ using the CCM89 reddening law (Table 5). We excluded $E(H-K_s)$ from this computation since we found a large systematic deviation of our color-excess estimates from the CCM89 law as discussed below.

In Figures 1–4 the best-fitting isochrones are overlaid on the cluster CMDs. While there is some variation in the quality of the data, we could divide the sample clusters into three groups based on how tight the MS is on optical CMDs. The

[5] Updated color transformations for 2MASS All-sky Data Release can be found at
http://www.ipac.caltech.edu/2mass/releases/allsky/doc/sec6_4b.html.

TABLE 5
COLOR-EXCESS RATIOS FOR ZERO-COLOR STARS

Color-Excess Ratios	CCM89[a]	BCP98[a]	This Paper[b]	Others[c]	ref
$E(V-I_C)/E(B-V)$	1.30	1.32	1.26 ± 0.06	1.25 ± 0.01	1
$E(V-K_s)/E(B-V)$	2.88	2.91	2.82 ± 0.06	2.78 ± 0.02	2,3,4
$E(J-K_s)/E(B-V)$	0.56	0.58	0.53 ± 0.04	0.52 ± 0.03	4
$E(H-K_s)/E(B-V)$	0.20	0.22	0.16 ± 0.02	0.20 ± 0.04	4

REFERENCES. — (1) Dean et al. 1978; (2) Schultz & Wiemer 1975; (3) Sneden et al. 1978; (4) Rieke & Lebofsky 1985.

NOTE. — Color excesses involving 2MASS JHK_s bandpasses are corrected for the difference in filter effective wavelengths.

[a]Estimated at $R_{V,0}$ = 3.26.

[b]Weighted mean and rms deviation.

[c]Revised for zero-color stars using color-dependent reddening relations in BCP98.

TABLE 6
MS-FITTING DISTANCE

Cluster	$(m-M)_0$								$(m-M)_{0,\rm ave}$[a]	$\sigma_{(m-M)}$[b]
	$(B-V,V)$	$N_{\rm fit}$	$(V-I_C,V)$	$N_{\rm fit}$	$(V-K_s,V)$	$N_{\rm fit}$	$(J-K_s,K_s)$	$N_{\rm fit}$		
NGC 129 .	11.030 ± 0.041	79	···	···	11.078 ± 0.044	58	11.007 ± 0.037	53	11.035 ± 0.023	0.027
VDB 1 ...	11.067 ± 0.097	20	10.744 ± 0.033	13	10.576 ± 0.062	13	10.706 ± 0.082	18	10.734 ± 0.026	0.209
NGC 5662	9.351 ± 0.025	52	···	···	9.290 ± 0.037	46	9.201 ± 0.043	37	9.307 ± 0.019	0.075
Lynga 6...	11.604 ± 0.114	21	11.415 ± 0.117	21	···	···	···	···	11.512 ± 0.082	0.134
NGC 6067	10.991 ± 0.019	141	11.125 ± 0.026	120	11.004 ± 0.033	43	10.996 ± 0.059	35	11.029 ± 0.013	0.064
NGC 6087	9.708 ± 0.048	22	···	···	9.601 ± 0.045	20	9.649 ± 0.049	19	9.650 ± 0.027	0.054
M25	8.961 ± 0.030	45	···	···	8.899 ± 0.054	36	8.885 ± 0.052	35	8.934 ± 0.023	0.040
NGC 7790	12.474 ± 0.014	63	12.427 ± 0.019	57	···	···	···	···	12.457 ± 0.011	0.033

NOTE. — Formal fitting errors are shown for individual distance moduli with a number of points used in the fit.

[a]Weighted average distance and its propagated error, not including systematic uncertainties.

[b]Standard deviation of individual distance moduli.

TABLE 7
MS-FITTING COLOR EXCESS

Cluster	$E(B-V)_0$	$N_{\rm fit}$	$E(V-I_C)_0$	$N_{\rm fit}$	$E(V-K_s)_0$	$N_{\rm fit}$	$E(J-K_s)_0$	$N_{\rm fit}$	$E(H-K_s)_0$	$N_{\rm fit}$	σ[a]
NGC 129 .	0.500 ± 0.008	53	···	···	1.431 ± 0.020	45	0.280 ± 0.006	43	0.069 ± 0.006	41	0.002
VDB 1 ...	0.573 ± 0.014	12	0.611 ± 0.023	9	1.458 ± 0.031	11	0.358 ± 0.013	10	0.066 ± 0.012	10	0.075
NGC 5662	0.277 ± 0.003	47	···	···	0.795 ± 0.012	41	0.172 ± 0.006	38	0.050 ± 0.005	37	0.018
Lynga 6...	1.326 ± 0.012	23	1.698 ± 0.017	22	3.659 ± 0.056	9	0.635 ± 0.020	8	0.200 ± 0.016	9	0.087
NGC 6067	0.340 ± 0.003	107	0.428 ± 0.007	67	0.935 ± 0.014	31	0.166 ± 0.008	26	0.025 ± 0.008	22	0.019
NGC 6087	0.132 ± 0.007	30	···	···	0.410 ± 0.010	25	0.084 ± 0.009	24	0.019 ± 0.007	24	0.009
M25	0.424 ± 0.009	60	···	···	1.160 ± 0.022	52	0.233 ± 0.007	47	0.077 ± 0.005	47	0.011
NGC 7790	0.509 ± 0.002	35	0.634 ± 0.005	33	1.457 ± 0.021	27	0.248 ± 0.010	28	0.110 ± 0.011	28	0.030

NOTE. — Color excess values are those for zero-color stars (see text). Formal fitting errors are shown for individual color excesses with a number of points used in the fit.

[a]Standard deviation of $E(B-V)$ estimates from all CMDs except $(H-K_s,K_s)$, after transforming color-excess values to $E(B-V)$ using the CCM89 color-excess ratios.

first group contains NGC 6067 and NGC 7790, which have well-populated CMDs and small fitting errors on each CMD. They also have a well-defined peak on the distribution of an individual star's distance modulus as shown in Figure 9 for NGC 7790. The second group is NGC 129, NGC 5662, Lynga 6, NGC 6087, and M25. These clusters have less well-defined peaks, either because of strong differential reddening (§ 5) or because of a bias in the sampling from photoelectric observations at faint magnitudes. The last group is VDB 1, which has a sparse MS and correspondingly large distance uncertainties.

We can also divide the clusters into groups by examining the difference in derived cluster properties from different colors. Clusters where the results from multi-color CMDs have a high internal consistency are strong cases, while clusters with substantial differences indicate problems. For the above first and second groups of clusters except Lynga 6, the standard deviations of individual distances [$\sigma_{(m-M)}$ in Table 6] are 0.03–0.08 mag, which are generally consistent with the fitting error on individual CMDs. On the other hand, both Lynga 6 and VDB 1 exhibit a larger dispersion in distance [$\sigma_{(m-M)}$ = 0.21 and 0.13 mag, respectively], and they also have a larger stan-

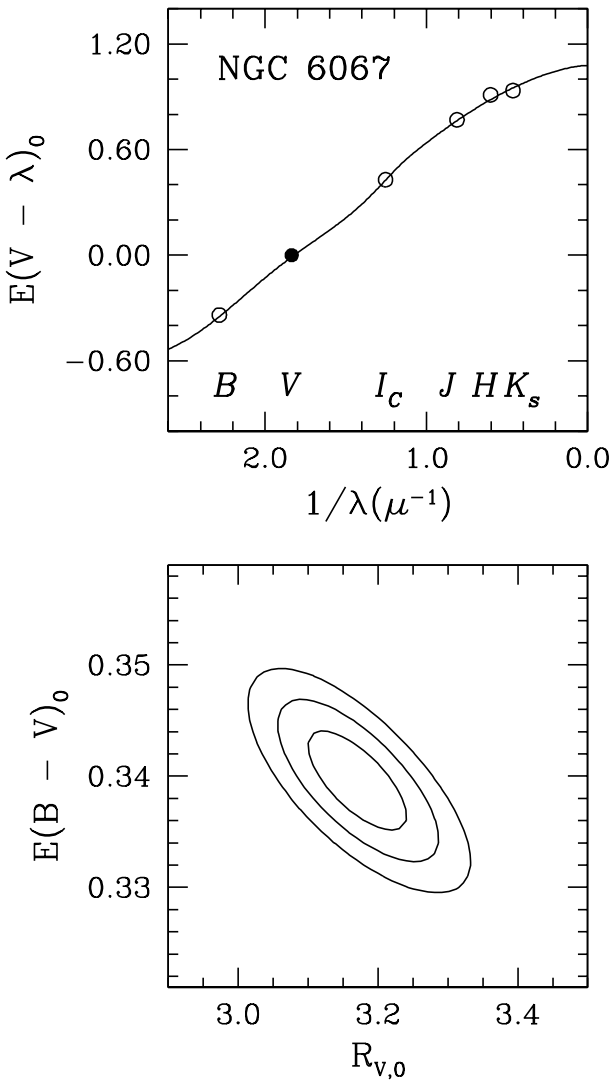


FIG. 8.— Example of determining $R_{V,0}$ and $E(B-V)_0$ for NGC 6067. *Top:* Solid line represents the best-fitting CCM89 extinction curve to color excesses (*open circles*). *Bottom:* Likelihood contours in $R_{V,0}$ and $E(B-V)_0$ shown at $\Delta\chi^2$ = 2.30, 6.17, and 11.8 (68.3%, 95.4%, and 99.73% confidence levels for 2 degrees of freedom).

dard deviation of $E(B-V)$ from different colors (σ in Table 7).

However, the dispersion in Lynga 6 is consistent with the statistical scatter expected from the small sample size. By contrast, VDB 1 has a statistically unreliable result that demands its exclusion from our data set. For this cluster, the best distance estimates inferred from different colors disagree by much more than their individual error estimates would imply. One possible explanation for the internal inconsistency is that the cluster MS is contaminated by less reddened field stars as shown by spectral-type study (Preston 1964). Because these stars happen to lie on the cluster MS, our photometric filtering could have misidentified cluster members. We therefore exclude VDB 1 from the following analysis and leave it for future studies.

Table 8 shows the error budget for NGC 6067 as an example. The first column displays individual sources of error, and the second column shows the size of the errors adopted for each quantity. The third through fifth columns list error contributions to $R_{V,0}$, $E(B-V)_0$, and $(m-M)_0$, respectively. The size of systematic errors in cluster metallicity, age, and pho-

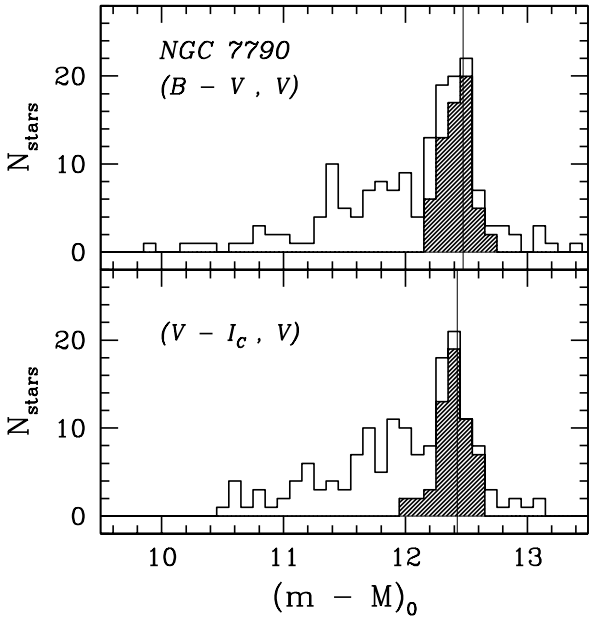


FIG. 9.— Distribution of individual distance moduli for NGC 7790 with respect to the isochrones shown in Fig. 1 and 2. The open histogram is the distribution of all stars in the isochrone fitting range where the distance was determined. The hatched histogram shows only for those that passed the photometric filtering. The vertical line indicates the weighted median distance modulus.

TABLE 8
ERROR BUDGET FOR NGC 6067

Source of Error	ΔQuantity	$\Delta R_{V,0}$	$\Delta E(B-V)_0$	$\Delta(m-M)_0$
[M/H].....	±0.05	±0.005	∓0.001	±0.056
logt (Myr)	±0.2	±0.009	∓0.013	∓0.020
Helium (ΔY)...	±0.010	···	···	∓0.030
$\Delta(B-V)$.....	±0.025	±0.264	∓0.022	∓0.007
$\Delta(V-I)_C$	±0.025	∓0.030	∓0.002	±0.027
ΔV	±0.025	∓0.085	±0.000	∓0.003
ΔJ.....	±0.011	±0.009	±0.000	∓0.001
ΔH	±0.007	±0.009	±0.000	∓0.002
ΔK_s	±0.007	±0.011	±0.000	∓0.005
Fitting.....	···	±0.061	±0.004	±0.032
Total	···	±0.286	±0.026	±0.079

NOTE. — $\Delta(B-V)$, $\Delta(V-I)_C$, ΔV, ΔJ, ΔH, and ΔK_s represent zero-point errors in the cluster photometry.

TABLE 9
SUMMARY OF CLUSTER PARAMETERS

Cluster	$R_{V,0}$	$E(B-V)_0$	$(m-M)_0$
NGC 129	3.31 ± 0.22	0.49 ± 0.03	11.04 ± 0.05
NGC 5662	3.30 ± 0.38	0.27 ± 0.03	9.31 ± 0.06
Lynga 6	3.16 ± 0.10	1.32 ± 0.03	11.51 ± 0.13
NGC 6067	3.18 ± 0.29	0.34 ± 0.03	11.03 ± 0.08
NGC 6087	3.59 ± 0.85	0.13 ± 0.03	9.65 ± 0.06
M25	3.16 ± 0.21	0.42 ± 0.03	8.93 ± 0.08
NGC 7790	3.18 ± 0.26	0.51 ± 0.02	12.46 ± 0.11

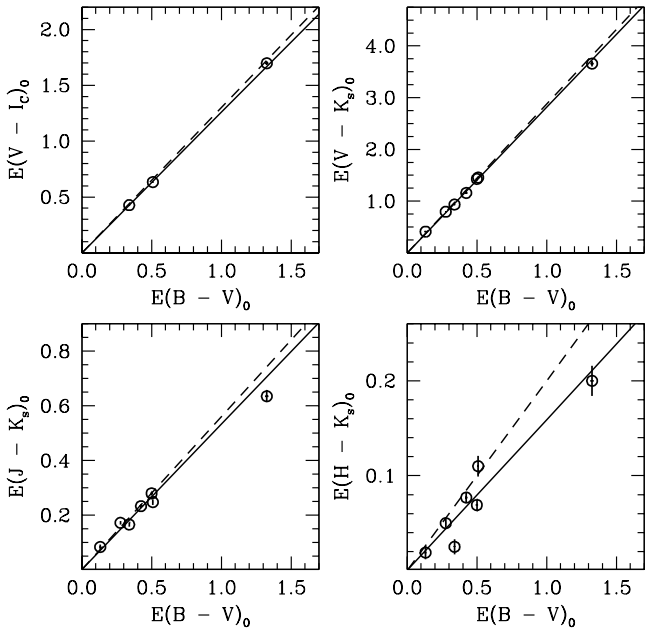


FIG. 10.— Mean color-excess ratios from the cluster sample. The error bars are from the isochrone fitting only. The solid line is a fit to the data, constrained to pass through the origin. The dashed line is the color-excess ratio from the CCM89 reddening law.

tometry was discussed in § 2. The quantity ΔY represents the uncertainty in the helium abundance at fixed metallicity and comes from the consideration of the initial solar abundance and those of the Hyades and the Pleiades (Paper I and Paper III). The fitting errors represent the internal precision of the fit and were taken as the larger value of the propagated error or $\sigma_{(m-M)}/\sqrt{N}$ in Table 6. We estimated the fitting errors in $R_{V,0}$ and $E(B-V)_0$ from the size of the 1σ contours on the $\Delta\chi^2$ distribution (e.g., Fig. 8). The total systematic error is the quadrature sum of these errors. The $R_{V,0}$, $E(B-V)_0$, and $(m-M)_0$ of our cluster sample are listed in Table 9 with total systematic errors in these quantities.

Independently of the CCM89 reddening law, we also derived color-excess ratios based on our cluster sample. Figure 10 shows a correlation between $E(B-V)$ and color-excess values in other color indices. Individual clusters are represented as a point, and fitting errors are shown only. The solid line is a linear fit to the data, constrained to pass through the origin. Table 5 summarizes our best-fit slopes of these lines or color-excess ratios. Our values are generally in good agreement with the CCM89 law and other observational estimates. However, our method yields a lower $E(H-K_s)/E(B-V)$ than these studies, which may reflect a zero-point offset in $H-K_s$ of our isochrones. Note that we did not derive color corrections for $H-K_s$.

4.2. *Comparison with Previous Studies*

The most up-to-date compilation of Cepheid parameters in open clusters and associations can be found in Tammann et al. (2003). Their distances are from the earlier compilation by Feast (1999). These ZAMS-fitting distances are the same as in Feast & Walker (1987), but include more recent distance estimates for NGC 129 (Turner et al. 1992) and NGC 7790 (Romeo et al. 1989). All of our Cepheids are listed in these tables, and the comparisons with distances in Feast & Walker and Tammann et al. are shown in the upper two panels of

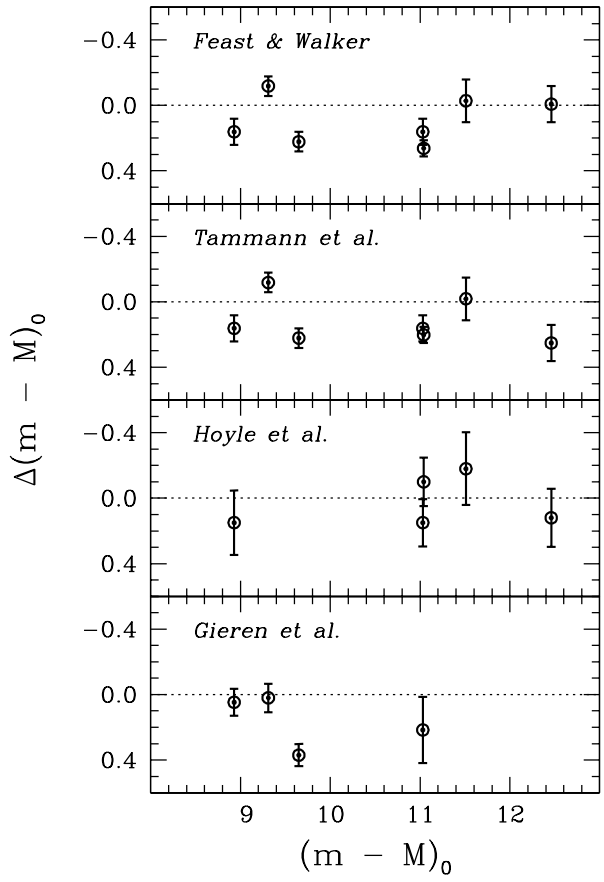


FIG. 11.— Comparison of cluster distances with those in Feast & Walker (1987), Tammann et al. (2003), Hoyle et al. (2003), and Gieren et al. (2005). The differences are in the sense of their distances minus those in this paper. The error bars are quadrature sum from the two studies in the lower two panels. Individual distances in the top two panels were revised assuming our Pleiades distance scale.

Figure 11 and listed in Table 10. Both of these studies estimated distances relative to the Pleiades but assumed different Pleiades distance of $(m-M)_0$ = 5.57 and 5.61 mag, respectively. We revised their distances assuming our Pleiades distance, $(m-M)_0$ = 5.63. Since they did not explicitly present errors, we plotted our errors only. The average differences in distance are $\Delta\langle(m-M)_0\rangle = 0.09 \pm 0.05$ and 0.12 ± 0.05 with Feast & Walker and Tammann et al., respectively. The sense of the differences is that our new distance estimates are shorter on average. The standard deviations of the differences are 0.14 mag for both comparisons, while the expected size from our error estimates is 0.07 mag. If our error estimates are correct, the dispersion indicates a random error of 0.12 mag in distance estimates from Feast & Walker and Tammann et al..

In addition to these studies, Hoyle et al. (2003) derived ZAMS-fitting distances to 11 open clusters with new photometry in *UBVK*. Our comparison with this study is shown in Figure 11 and tabulated in Table 10. The error bars represent quadrature sums of our and their reported error estimates. Their distances are marginally consistent with our estimates, and the average difference is $\Delta\langle(m-M)_0\rangle = 0.04 \pm 0.07$, our distances being shorter on average. However, we did not attempt to revise their distances assuming our Pleiades distance scale. They used a ZAMS from Allen (1973) for the optical data, but they also claimed that the same results were obtained from the ZAMS in Turner (1979) and Mermilliod

TABLE 10
COMPARISON OF CLUSTER DISTANCE WITH PUBLISHED RESULTS

Cluster	This Study	FW87[a]	TSR03[a]	HST03	G05[b]
NGC 129 .	11.04 ± 0.05	11.30	11.24	10.94 ± 0.14	···
NGC 5662	9.31 ± 0.06	9.19	9.19	···	9.33 ± 0.06
Lynga 6...	11.51 ± 0.13	11.48	11.49	11.33 ± 0.18	···
NGC 6067	11.03 ± 0.08	11.19	11.19	11.18 ± 0.12	11.25 ± 0.19
NGC 6087	9.65 ± 0.06	9.87	9.87	···	10.02 ± 0.03
M25	8.93 ± 0.08	9.09	9.09	9.08 ± 0.18	8.98 ± 0.02
NGC 7790	12.46 ± 0.11	12.45	12.71	12.58 ± 0.14	···

NOTE. — FW87, Feast & Walker (1987); TSR03, Tammann et al. (2003); HST03, Hoyle et al. (2003); G05, Gieren et al. (2005).

[a]Distances revised assuming the same Pleiades distance, $(m-M)_0 = 5.63$, as in this paper.
[b]Distances to individual Cepheids from the surface brightness technique.

(1981). Since the Pleiades distance modulus of 5.56 mag was adopted in Turner, the distance moduli in Hoyle et al. would then become longer by ≈ 0.07 mag on average than ours when they are on the same Pleiades distance scale as in this paper.

The bottom panel in Figure 11 shows the comparison with distances from the surface brightness technique by Gieren et al. (2005). Their distances are also larger on average than our estimates by 0.15 ± 0.09 mag as in the previous MS-fitting studies. However, they recalibrated the projection factor, which was used to convert observed velocities to pulsational velocities, using MS-fitting distances to cluster Cepheids. Therefore, their estimates are not completely independent from the above MS-fitting studies.

Our short distances are mainly due to our lower $E(B-V)$ values than those in the previous work. This is because the MS-fitting distances are correlated with reddening by $\Delta(m-M)_0/E(B-V) \sim 2$ (Paper III). The top panel in Figure 12 compares the Cepheid reddening with those in Feast & Walker (1987), and individual estimates are listed in Table 11. They estimated the OB star reddening at the location of the Cepheids and then transformed it to the value appropriate for the Cepheid using a color-dependent reddening law (e.g., eqs. [2] and [3]). The mean difference from our study is $\langle E(B-V) \rangle = 0.04 \pm 0.02$ mag, our values being smaller on average. The difference in $E(B-V)$ then approximately matches the size expected to produce the difference in distance modulus (~ 0.1 mag).

Individual reddening estimates from Fernie et al. (1995), Tammann et al. (2003), and Hoyle et al. (2003) are also listed in Table 11, and comparisons with our estimates are shown in Figure 12. Many studies used an extensive compilation of Cepheid reddening in the David Dunlap Observatory (DDO) database of Galactic classical Cepheids,[6] which is from heterogeneous methods (Fernie 1990, 1994; Fernie et al. 1995). The mean difference with their data is $\Delta\langle E(B-V) \rangle = 0.05$ in the sense that our reddening is smaller. Tammann et al. adopted these reddening estimates for their cluster Cepheids but made slight corrections to remove a mild correlation of the color excess with residuals from the period-color relation. This results in a reduced difference with our estimates by $\Delta\langle E(B-V) \rangle = 0.02$. However, the results from Tammann et al. are internally less consistent, in the sense that the extinction corrections on the Cepheid magnitudes and the reddening values for the MS-fitting distance estimates were not derived from the same methods. Finally, we compared our reddening values with those in Hoyle et al., which were based on the cluster *UBV* color-color diagram. Their values are also systematically larger than ours by $\Delta\langle E(B-V) \rangle = 0.04 \pm 0.01$.

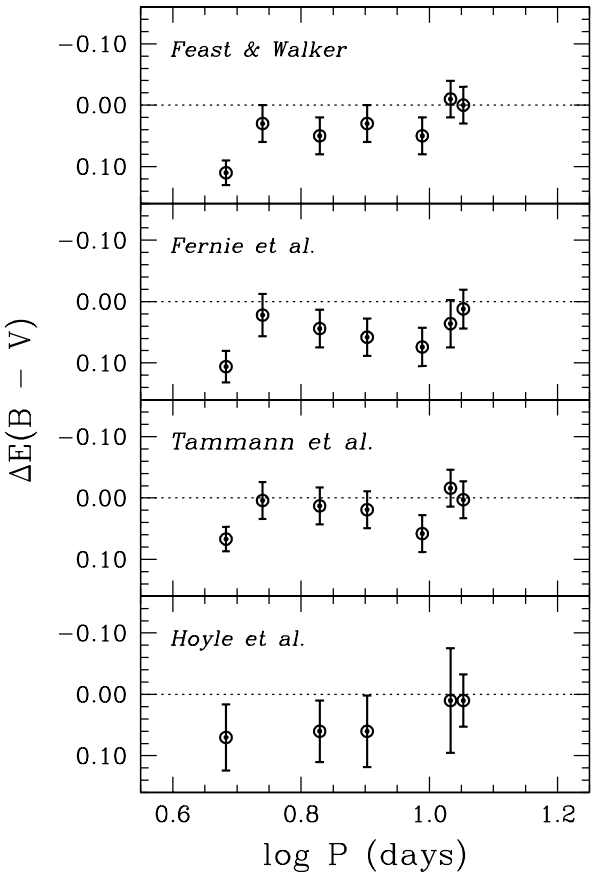


FIG. 12.— Comparison of Cepheid $E(B-V)$ with those in Feast & Walker (1987), Fernie et al. (1995), Tammann et al. (2003), and Hoyle et al. (2003). The differences are in the sense of their values minus those in this paper. Error bars represent our error estimates in the top three panels, but they show a quadrature sum from two studies in the bottom panel (Hoyle et al.).

There are a limited number of reddening estimates from the spectral types in the literature. Kraft (1958) estimated $E(B-V) = 0.45$ from one B-type star in NGC 129, while Arp et al. (1959) found $\langle E(B-V) \rangle = 0.53 \pm 0.01$ from seven stars in the vicinity of its Cepheid (DL Cas). In M25, Sandage (1960) estimated $\langle E(B-V) \rangle = 0.43 \pm 0.05$ from the spectral types given by Feast (1957) and 0.43 ± 0.06 by Wallerstein

[6] http://www.astro.utoronto.ca/DDO/research/cepheids/

TABLE 11
COMPARISON OF CEPHEID $E(B-V)$ WITH PUBLISHED RESULTS

Cluster	This Study[a]	FW87	F95	TSR03	HST03
NGC 129 .	0.46 ± 0.03	0.49	0.52 ± 0.01	0.48	0.52 ± 0.05
NGC 5662	0.26 ± 0.03	0.29	0.28 ± 0.02	0.26	...
Lynga 6 ...	1.23 ± 0.03	1.22	1.27 ± 0.02	1.21	1.24 ± 0.08
NGC 6067	0.32 ± 0.03	0.32	0.33 ± 0.01	0.32	0.33 ± 0.03
NGC 6087	0.12 ± 0.03	0.17	0.19 ± 0.01	0.18	...
M25	0.39 ± 0.03	0.44	0.43 ± 0.01	0.40	0.45 ± 0.04
NGC 7790[b]	0.48 ± 0.02	0.59	0.59 ± 0.02	0.55	0.55 ± 0.05

NOTE. — FW87, Feast & Walker (1987); F95, Fernie et al. (1995); TSR03, Tammann et al. (2003); HST03, Hoyle et al. (2003).

[a] Errors from differential reddening are not included.
[b] Average value for CEa Cas, CEb Cas, and CF Cas.

(1957), but found a slightly larger reddening, 0.46 ± 0.04, in the vicinity of its Cepheid (U Sgr). Finally, Kraft (1958) estimated $\langle E(B-V) \rangle = 0.49 \pm 0.02$ from six stars in NGC 7790. These estimates are generally found between the previous estimates and our new values. Because of low Galactic latitudes of the clusters ($|b| < 5°$), the dust map of Schlegel et al. (1998) could not provide meaningful upper limits on the color excess.

We contend that our reddening estimates are more reliable than the previous values, which mostly relied on the solar metallicity ZAMS-fitting on *UBV* color-color diagrams. In contrast to these studies, we took into account metallicity and age effects on MS fitting, and our estimates are based on simultaneous fits over a wider range of spectral bands, including near-infrared JHK_s. We also note that photometric zero-point errors in *U*-band (e.g., Bessell 2005) could introduce significant uncertainties in color excesses derived from *UBV* color-color diagrams.

5. GALACTIC PERIOD-LUMINOSITY RELATIONS

With cluster parameters derived in the previous section, we are now in a position to estimate absolute magnitudes of Cepheids and to redetermine the Galactic *P-L* relations. We show that our new *P-L* relation in *V* is generally fainter than in previous studies. However, it is in good agreement with recent parallax studies (Benedict et al. 2007; van Leeuwen et al. 2007) when the Wesenheit magnitudes are employed.

5.1. *Absolute Magnitudes of Cepheids*

The absolute *V* magnitude was computed for each Cepheid from

$$\langle M_V \rangle = \langle m_V \rangle - (m-M)_0 - R_V E(B-V), \qquad (10)$$

where $\langle m_V \rangle$ is the observed intensity-mean magnitude and $(m-M)_0$ is the extinction-corrected distance modulus. We used the same color-dependent prescriptions for R_V and $E(B-V)$ as those for MS dwarfs (eqs. [2] and [3]). The absolute magnitudes in other filter passbands were computed from the CCM89 reddening law at each cluster's $R_{V,0}$. Table 12 lists absolute magnitudes in BVI_CJHK_s for all Cepheids in this study. In the last column we also show the reddening-insensitive Wesenheit magnitude, $\langle W_{VI} \rangle \equiv \langle V \rangle - 2.45(\langle V \rangle - \langle I_C \rangle)$, which was adopted in the *HST* Key Project.[7]

Table 13 shows systematic errors in $\langle M_V \rangle$ of the Cepheids. As in Table 8, we estimated the size of errors by performing MS fits for alternate values of systematic error quantities. These are shown in the first and second columns, which are the same as those in Table 8 except the last two rows: Δm_V and $\sigma_{E(B-V)}$. The Δm_V represents a systematic error in the Cepheid photometry, which was treated as independent of the cluster photometry and any of the MS-fitting process. Note that $(m-M)_0$, R_V, and $E(B-V)$ in equation (10) are correlated with each other via MS fitting.

The $\sigma_{E(B-V)}$ in Table 13 represents the error in the reddening for individual Cepheids. In equation (10) we adopted the Cepheid reddening as the mean cluster reddening value. However, reddening for individual stars becomes more uncertain as we deal with more differentially reddened clusters. For these clusters, the colors for individual stars scatter along a reddening vector, and this can be detected by a large size of the MS width above photometric precision.

To estimate the size of differential reddening for each cluster, we first computed the standard deviation of $B-V$ colors in the upper MS from Table 7. Since the photometric filtering likely reduces the size of the dispersion, we corrected for it from artificial cluster CMD tests (Paper III). We generated solar metallicity, 80 Myr isochrones with photometric errors of 0.02 mag in colors and magnitudes. We used the Salpeter (1955) mass function for the primaries and a flat mass function for the secondaries for a 40% binary fraction.[8] Single stars and binaries were then randomly displaced from the MS assuming a normal distribution of individual reddening with a standard deviation $\sigma_{E(B-V)}$. After applying the photometric filtering, we then estimated the size of the reduction in dispersion as a function of $\sigma_{E(B-V)}$. In this way, we inferred $\sigma_{E(B-V)}$ for each cluster from the observed dispersion in $B-V$, which are shown in the second column of Table 14. We made no corrections to those for NGC 5662 and NGC 7790 because the dispersions in $B-V$ were equal to or smaller than our assumed photometric precision ($\sigma_{B-V} = 0.02$).

In addition to previously known clusters with differential reddening (NGC 129, NGC 5662, and M25), we also found

[7] We simply adopted $A_V/E(V-I_C) = 2.45$ from Freedman et al. (2001) to directly compare our results with those of other studies, which also employed the same relation. We would derive $A_V/E(V-I_C) = 2.56$ for the Cepheids with $\langle B_0 \rangle - \langle V_0 \rangle = 0.7$ at $R_V = 3.35$, computed from the average $R_{V,0}$ of our cluster sample. This difference in $A_V/E(V-I_C)$ has a negligible effect on W_{VI} of Cepheids. It is noted that Macri et al. (2001b) tested the CCM89 reddening law using *VIH* photometry for 70 extragalactic Cepheids in 13 galaxies. They showed that a mean color-excess ratio of $E(V-H)/E(V-I)$ is in good agreement with the CCM89 predicted value.

[8] The binary fraction is defined as the number of binaries divided by the total number of systems in the considered fitting range.

TABLE 12
CEPHEID ABSOLUTE MAGNITUDES

Cepheids	log P	$\langle M_B \rangle$	$\langle M_V \rangle$	$\langle M_{I_C} \rangle$	$\langle M_J \rangle$	$\langle M_H \rangle$	$\langle M_{K_s} \rangle$	$\langle M_{W(VI)} \rangle$[a]
DL Cas ..	0.903	–2.988	–3.673	–4.364	···	···	···	–5.285
V Cen ...	0.740	–2.754	–3.371	–4.042	–4.557	–4.848	–4.951	–4.974
TW Nor .	1.033	–3.187	–3.957	–4.716	–5.287	–5.580	–5.775	–5.676
V340 Nor	1.053	–2.879	–3.720	–4.505	–5.142	–5.500	–5.641	–5.604
S Nor ...	0.989	–2.864	–3.685	–4.518	–5.128	–5.470	–5.593	–5.688
U Sgr ...	0.829	–2.829	–3.535	–4.270	–4.794	–5.086	–5.196	–5.294
CEa Cas .	0.711	–2.458	–3.129	–3.951	···	···	···	–5.090
CEb Cas .	0.651	–2.306	–2.998	–3.731	···	···	···	–4.739
CF Cas ..	0.688	–2.189	–2.911	–3.667	···	···	···	–4.707

[a]Wesenheit index from Freedman et al. (2001): $\langle W(VI) \rangle \equiv \langle V \rangle - 2.45(\langle V \rangle - \langle I_C \rangle)$.

TABLE 13
ERROR BUDGET IN $\langle M_V \rangle$

Source of Error	ΔQuantity	NGC 129 DL Cas	NGC 5662 V Cen	Lynga 6 TW Nor	NGC 6067 V340 Nor	NGC 6087 S Nor	M25 U Sgr	NGC 7790 CEa, CEb, CF Cas
[M/H][a]	···	$\mp$0.032	$\mp$0.028	$\mp$0.056	$\mp$0.054	$\mp$0.028	$\mp$0.045	$\mp$0.054
logt (Myr)	$\pm$0.2	$\pm$0.037	$\pm$0.007	$\mp$0.014	$\pm$0.057	$\pm$0.061	$\pm$0.051	$\pm$0.021
Helium (ΔY)...	$\pm$0.010	$\mp$0.030	$\mp$0.030	$\mp$0.030	$\mp$0.030	$\mp$0.030	$\mp$0.030	$\mp$0.030
$\Delta(B-V)$.....	$\pm$0.025	$\mp$0.009	$\mp$0.001	$\pm$0.014	$\mp$0.007	$\mp$0.002	$\mp$0.002	$\pm$0.001
$\Delta(V-I)_C$	$\pm$0.025	···	···	···	$\mp$0.012	···	···	$\mp$0.011
ΔV	$\pm$0.025	$\pm$0.048	$\pm$0.025	$\pm$0.028	$\pm$0.030	$\pm$0.022	$\pm$0.013	$\pm$0.026
ΔJ	$\pm$0.011	$\mp$0.014	$\mp$0.004	$\mp$0.002	$\mp$0.003	$\mp$0.005	$\mp$0.005	$\pm$0.000
ΔH	$\pm$0.007	$\pm$0.001	$\mp$0.001	$\mp$0.002	$\mp$0.001	$\mp$0.002	$\mp$0.002	$\pm$0.001
ΔK_s	$\pm$0.007	$\pm$0.010	$\pm$0.002	$\mp$0.002	$\pm$0.002	$\pm$0.004	$\pm$0.004	$\mp$0.001
Fitting	···	$\pm$0.023	$\pm$0.044	$\pm$0.094	$\pm$0.032	$\pm$0.031	$\pm$0.040	$\pm$0.023
Δm_V[b]	$\pm$0.025	$\pm$0.025	$\pm$0.025	$\pm$0.025	$\pm$0.025	$\pm$0.025	$\pm$0.025	$\pm$0.025
$\sigma_{E(B-V)}$[c]	···	$\pm$0.347	$\pm$0.066	$\pm$0.316	$\pm$0.159	$\pm$0.197	$\pm$0.379	$\pm$0.041
Total	···	$\pm$0.357	$\pm$0.097	$\pm$0.338	$\pm$0.187	$\pm$0.216	$\pm$0.390	$\pm$0.089

NOTE. — $\Delta(B-V)$, $\Delta(V-I)_C$, ΔV, ΔJ, ΔH, and ΔK_s represent zero-point errors in the cluster photometry.

[a]Individual errors taken from Table 1.
[b]Photometric zero-point error in the intensity mean magnitude of a Cepheid.
[c]Differential reddening over a cluster field.

TABLE 14
RESULTS FROM ARTIFICIAL CLUSTER TESTS

Cluster	$\sigma_{E(B-V)}$[a]	$\Delta\langle M_V \rangle$[b]
NGC 129 .	0.105	$+0.04 \pm 0.14$
NGC 5662	0.020[c]	-0.06 ± 0.05
Lynga 6...	0.100	$+0.04 \pm 0.14$
NGC 6067	0.050	-0.06 ± 0.07
NGC 6087	0.055	-0.06 ± 0.08
M25	0.120	$+0.02 \pm 0.15$
NGC 7790	0.013[c]	-0.05 ± 0.04

[a]Size of differential reddening inferred from artificial cluster tests, assuming a normal distribution of $E(B-V)$.
[b]This value should be subtracted from the estimated $\langle M_V \rangle$. Errors are semi-interquartile ranges.
[c]Not corrected from the artificial cluster tests.

that the remaining clusters except NGC 7790 have larger dispersions than photometric errors. While this could be due to remaining binaries, background stars, rapid rotators, or an underestimation of the photometric errors, we took the excess dispersion in Table 14 as a characteristic measure of differential reddening as a conservative error estimate. The $\sigma_{E(B-V)}$ in Table 14 was then multiplied by R_V to estimate the error in $\langle M_V \rangle$, which is shown in Table 13. For all clusters except NGC 7790, differential reddening is the largest error source in $\langle M_V \rangle$.

In previous studies, local Cepheid reddening was often determined using photometry of neighboring stars. We experimented with this approach for M25. We estimated individual Cepheid's reddening on $(B-V,V)$ and assumed that the dispersion around the best-fitting isochrone is solely due to differential reddening. However, we could not place a strong constraint on the local color excess for U Sgr because there were not a sufficient number of stars with good $E(B-V)$. In addition, cluster binaries cannot be easily distinguished from highly reddened single stars on CMDs, which could lead to an overestimation of reddening.

5.2. *The Galactic P-L Relations*

Our Cepheid sample does not span a wide range of periods, which leads to a large error in *P-L* slopes. Instead, we adopted the *P-L* slopes derived from LMC Cepheids, assuming that the *P-L* relations for Cepheids in the Galaxy and in the LMC have the same slopes. Some investigators have claimed that

the Galactic *P-L* relations are steeper than those of the LMC Cepheids, and that the LMC *P-L* relations have a break at $P \approx 10$ days, possibly due to different metal contents of Cepheids (Kanbur & Ngeow 2004; Sandage et al. 2004; Ngeow et al. 2005). However, Macri et al. (2006) recently showed that *P-L* relations from the LMC Cepheids in the OGLE-II catalog (Udalski et al. 1999a) are a good fit to Cepheids in the two fields of NGC 4258, which have approximately the LMC and the Galactic metal abundances (see § 6.1).

We derived LMC *P-L* slopes using fundamental mode Cepheids in the OGLE-II catalog (Udalski et al. 1999a) and those in Persson et al. (2004). The OGLE-II Cepheids have an average period of $\langle \log P(\text{days}) \rangle \approx 0.6$ with about half of them being in the same period range as our Galactic Cepheid sample. The *P-L* relations in the LMC from the OGLE-II database were originally derived by Udalski et al. (1999b) and then revised according to the new photometric calibration (Udalski 2000). We rederived the period-*apparent* magnitude relations in BVI_C using the revised data from the OGLE-II Internet archive[9] after iterative 2.5σ rejection from 680 Cepheids with $\log P > 0.4$ (Udalski et al. 1999b). We also derived similar relations in JHK_s on the LCO system from the photometry in Persson et al. (2004). As in their analysis, we excluded four stars (HV 883, HV 2447, and HV 2883 have periods longer than 100 days, and HV 12765 is about 0.2 mag brighter than the mean *P-L* relation), leaving 88 Cepheids with $\log P > 0.4$.

We then derived the Galactic *P-L* relations in BVI_CJHK_s after correcting for interstellar extinction:

$$\langle M_B \rangle = (-3.169 \pm 0.085) - (2.503 \pm 0.048)(\log P - 1),$$
$$\langle M_V \rangle = (-3.932 \pm 0.066) - (2.819 \pm 0.032)(\log P - 1),$$
$$\langle M_{I_C} \rangle = (-4.712 \pm 0.057) - (3.004 \pm 0.021)(\log P - 1),$$
$$\langle M_J \rangle = (-5.271 \pm 0.076) - (3.148 \pm 0.053)(\log P - 1),$$
$$\langle M_H \rangle = (-5.593 \pm 0.069) - (3.233 \pm 0.044)(\log P - 1),$$
$$\langle M_{K_s} \rangle = (-5.718 \pm 0.064) - (3.282 \pm 0.040)(\log P - 1).$$

The slope errors are those estimated from the LMC Cepheids. The zero-point errors were estimated from the magnitude dispersion among the Cepheids, assuming that the magnitude errors are uncorrelated with each other. We took the average magnitudes and periods of the three Cepheids in NGC 7790 as one data point. Cepheids in the two northern clusters (NGC 129 and NGC 7790) have no photometry in Laney & Stobie (1992), so the *P-L* relations in JHK_s were derived from five clusters.

Figures 13 and 14 display *P-L* relations for our Galactic Cepheids (*bull's-eyes*) in all filter passbands. In *V*-band the χ^2 of the fit is 8.0 for 6 degrees of freedom, which indicates our reasonable error estimation. The standard deviation of the Galactic Cepheids around the *P-L* relation is 0.18 mag, which is comparable to that of the LMC counterparts (Udalski et al. 1999b). This value is smaller than previous estimates for the Galactic Cepheids from MS fitting: Tammann et al. (2003) found 0.26 mag for 25 Cepheids (see also Sandage et al. 2004), and Fouqué et al. (2003) estimated 0.27 mag from 24 Cepheids.

In Figure 13 the OGLE-II Cepheids are also shown at a distance modulus of 18.50 mag, which was adopted in the *HST* Key Project (*small boxes*). Magnitudes of these Cepheids were corrected for extinction based on the OGLE-II reddening map, which was derived from the I_C-band magnitudes of red clump stars (Udalski et al. 1999a). As seen in the figure, the

[9] http://www.astrouw.edu.pl/~ogle/ogle2/cep_lmc.html

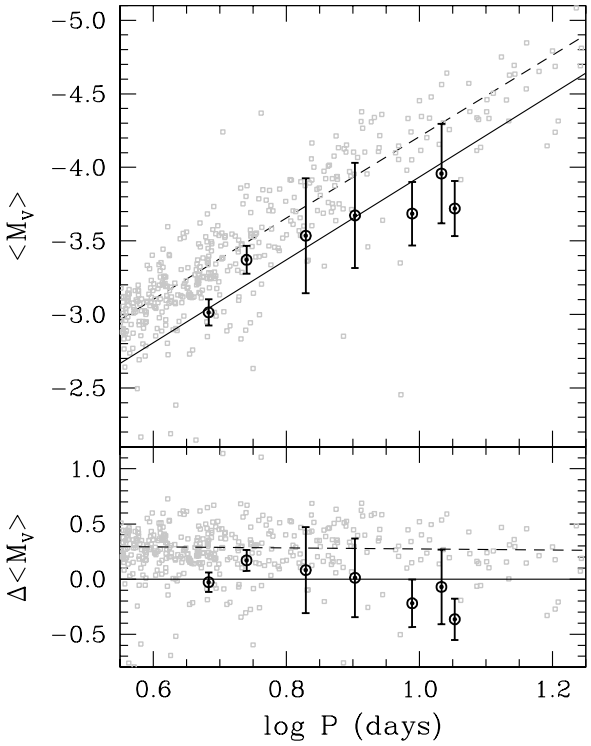


FIG. 13.— Galactic *P-L* relation in *V*. The bull's-eyes are our Galactic calibrators with their 1σ errors, and the solid line is a fit to these points assuming the LMC *P-L* slope. The small boxes are LMC fundamental mode Cepheids from the OGLE-II survey, assuming $(m-M)_0 = 18.50$ and the OGLE-II reddening map. The dashed line is a fit to these points.

LMC *P-L* relation (*dashed line*) is brighter than our Galactic *P-L* relation (*solid line*) by ~ 0.3 mag. This is due to metallicity and reddening effects, as well as the LMC distance as discussed in § 6.2.

5.3. *Comparison with Previous Studies*

Figure 15 compares our $\langle M_V \rangle$ with those of Feast & Walker (1987), Tammann et al. (2003), Hoyle et al. (2003), and Gieren et al. (2005). Error bars represent our error estimates only. We revised absolute magnitudes in Feast & Walker and Tammann et al. assuming our Pleiades distance (5.63 mag in distance modulus). Individual $\langle M_V \rangle$ estimates are shown in Table 15. We restricted our comparison to $\langle M_V \rangle$ since absolute magnitudes in other passbands are correlated with each other. The weighted average differences are $\Delta\langle M_V \rangle = -0.17 \pm 0.07$, -0.09 ± 0.09, -0.14 ± 0.10, and -0.22 ± 0.11 from Feast & Walker, Tammann et al., Hoyle et al., and Gieren et al., respectively, in the sense that our estimates are fainter on average. This is mainly due to the fact that our distance and reddening estimates are smaller on average than those in the previous studies (§ 4.2).

In addition, we also made a comparison with all cluster Cepheids in Tammann et al. (2003) as shown in the left panel of Figure 16. As found in the above Cepheid-to-Cepheid comparison, the difference with their $\langle M_V \rangle$ is statistically insignificant for Cepheids with $\log P \lesssim 1.1$. However, their *P-L* relation is steeper than ours because their long-period Cepheids at $\log P \gtrsim 1.1$ are brighter than expected from our *P-L* relation. If we assume their *P-L* slope for our sample, we would derive $\langle M_V \rangle = -4.01$ for 10-day period Cepheids, which is 0.25 mag fainter than their *P-L* zero point.

In the right panel of Figure 16, we compare our Galac-

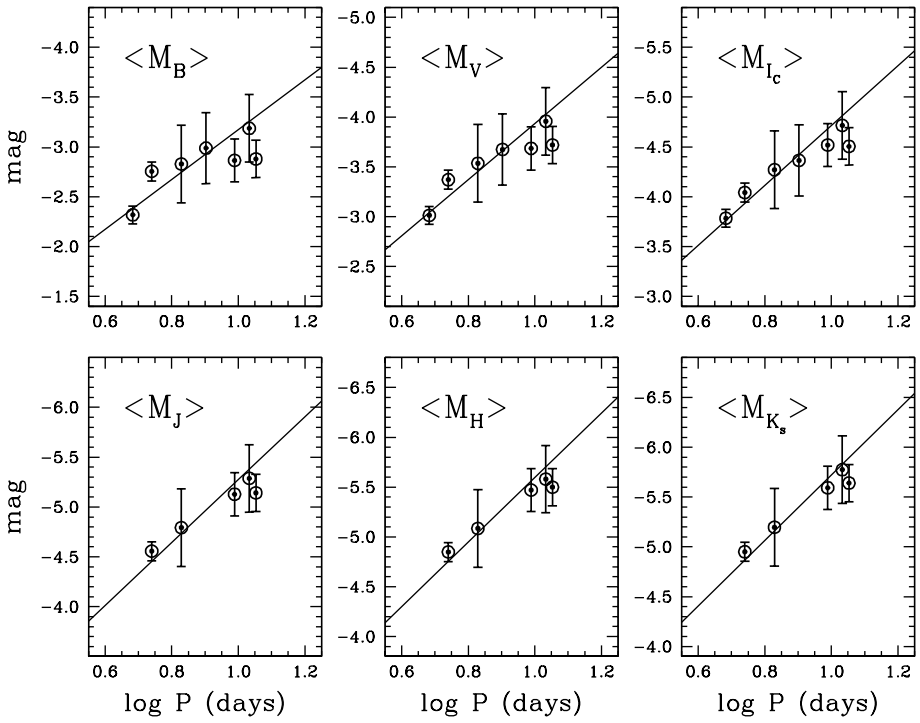


FIG. 14.— Same as Fig. 13, but in all BVI_CJHK_s.

TABLE 15
COMPARISON OF CEPHEID $\langle M_V \rangle$ WITH PUBLISHED RESULTS

Cluster	This Study	FW87[a]	TSR03[a]	HST03	G05
DL Cas	-3.67 ± 0.36	–3.92	–3.77	–3.69	···
V Cen	-3.37 ± 0.10	–3.30	–3.19	···	–3.45
TW Nor	-3.96 ± 0.34	–3.85	–3.72	–3.79	···
V340 Nor	-3.72 ± 0.19	–3.86	–3.85	–3.92	–3.91
S Nor	-3.69 ± 0.22	–4.01	–4.00	···	–4.21
U Sgr	-3.54 ± 0.39	–3.83	–3.66	–3.88	–3.62
CEa,CEb,CF Cas[b]	-3.01 ± 0.09	–3.36	–3.37	–3.34	···

NOTE. — FW87, Feast & Walker (1987); TSR03, Tammann et al. (2003); HST03, Hoyle et al. (2003); G05, Gieren et al. (2005).

[a]Magnitudes revised assuming the same Pleiades distance, $(m-M)_0 = 5.63$, as in this paper.
[b]Average value for CEa Cas, CEb Cas, and CF Cas.

tic *P-L* relation in *V* with that of the recent *HST* parallax study (Benedict et al. 2007), which provided accurate parallaxes (average 8%) for nine Galactic Cepheids using the *HST* Fine Guidance Sensor (see also Benedict et al. 2002b). Their Cepheid parallaxes were estimated with respect to photometric parallaxes of reference stars, which set the absolute distance scale of each reference frame. The magnitudes were then corrected for interstellar extinction from either color-color relations or the DDO Galactic Cepheid database. We have no Cepheids in common with their study since their distance measurements were focused on nearby field Cepheids. If we assume their *P-L* slope, our 10-day period Cepheids would be 0.20 mag fainter than their zero point. If the difference is solely due to the error in our reddening estimates, our estimates would have been underestimated by $\Delta\langle E(B-V)\rangle \sim 0.04$. However, it is noted that reddening can be determined far more accurately for cluster Cepheids than it can for field stars. Our error bars in Figure 16 are slightly larger than those of the *HST* study because of our conservative error estimates for the extinction correction.

On the other hand, the *HST*-based *P-L* relation is in better agreement with ours when the Wesenheit magnitude $W(VI)$ is used as shown in Figure 17. The weighted mean difference of our Galactic Cepheids from their best-fitting *P-L* relation (*solid line*) is $\Delta\langle M_{W(VI)}\rangle = 0.05 \pm 0.06$ in the sense that our *P-L* relation is fainter. Since the Wesenheit magnitude was designed to minimize the effect of errors in the reddening, the agreement may indicate that the large difference in $\langle M_V \rangle$ is due to the difference in the distance estimation.

Previous studies based on *Hipparcos* data typically yielded $\langle M_V \rangle \approx -4.2$ for 10-day period Cepheids (Feast & Catchpole 1997; Feast et al. 1998; Lanoix et al. 1999; Groenewegen & Oudmaijer 2000), while Luri et al. (1998) obtained $\langle M_V \rangle \approx -3.9$ from statistical parallaxes. Recently, van Leeuwen et al. (2007) reexamined the Galactic *P-L* relations based on the new reduction of the *Hipparcos* astrometric data (van

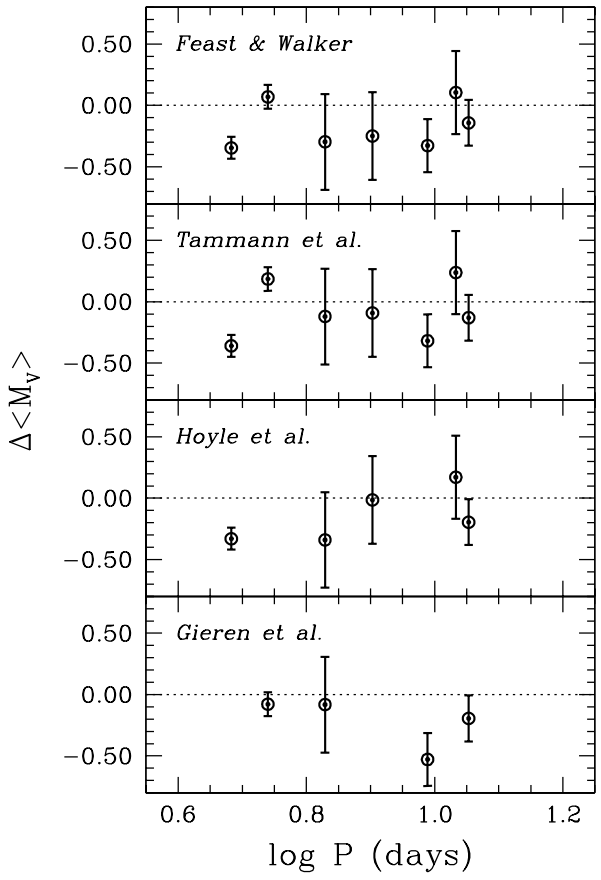


FIG. 15.— Comparison of Cepheid absolute magnitudes with those in Feast & Walker (1987), Tammann et al. (2003), Hoyle et al. (2003), and Gieren et al. (2005). The differences are in the sense of their magnitudes minus those in this paper. The error bars represent our error estimates only. Individual $\langle M_V \rangle$ estimates in the top two panels were revised assuming our Pleiades distance scale.

TABLE 16
ERROR BUDGET IN $\langle M_V \rangle$ FOR 10-DAY PERIOD CEPHEIDS FROM MS FITTING

Source of Error	$\Delta\langle M_V \rangle$
Isochrone Calibration.....	±0.02
Metallicity Scale (±0.1 dex)	±0.11
Age Scale [$\Delta \log t$(Myr) = ±0.2] ..	±0.03
Reddening Laws.....	±0.05
Differential Reddening + Binary	±0.05
Total Systematic.....	±0.14
Statistical	±0.07
Combined (Systematic + Statistical)	±0.16

Leeuwen & Fantino 2005), where improvements of up to a factor of 2 in parallax accuracy have been achieved by reconstructing the satellite's attitude (van Leeuwen 2005). They analyzed their data together with the *HST* parallaxes to derive a *P-L* relation in $W(VI)$. If we adopt their *P-L* slope in $W(VI)$, our *P-L* relation would be $\Delta\langle M_{W(VI)} \rangle = 0.07 \pm 0.06$ fainter than their best-fitting *P-L* relation.

5.4. *Systematic Errors in P-L relations*

When determining the *P-L* relations in the previous section, we assumed that the errors in $\langle M_V \rangle$ of individual Cepheids (Table 13) are uncorrelated with each other. However, there are a number of error sources that could systematically change $\langle M_V \rangle$. These are shown in Table 16 with their estimated size of error contributions to the *P-L* zero point, which is described below in detail. In short, the calibration error is from the uncertainty in the adopted distance of the Pleiades (Paper III). Errors in the metallicity scale of ±0.1 dex and the age scale of $\Delta \log t$(Myr) = 0.2 were adopted. The error from the reddening laws represents the case of using different color-dependent prescriptions for $E(B-V)$ and R_V from Feast & Walker (1987) and Laney & Stobie (1993). We performed artificial cluster CMD tests to estimate a probable size of a bias in the MS-fitting technique from differential reddening and unresolved cluster binaries.

From the comparison with Yong et al. (2006) and Andrievsky et al. (2002), we inferred that our adopted metallicity scale (Fry & Carney 1997) has a 0.1 dex systematic error (§ 2.1). Metallicity changes of ±0.1 dex would vary the $\langle M_V \rangle$ of 10-day period Cepheids from –3.84 to –4.04 mag.

In this paper, only the relative age scale is relevant with respect to the Pleiades. Our assumed age range in § 2.1 reflects the cluster-to-cluster variations with respect to the adopted age of 80 Myr. However, it is possible that the Cepheid clusters are all systematically younger or older than the Pleiades. This would change the reddening values since the mean color of the upper MS varies with the cluster age. In fact, some of the CMDs have stars that extend far above the top end of the 80 Myr isochrone. If these bright stars are cluster members, they would suggest younger ages than 80 Myr. Nevertheless, the *P-L* zero point is relatively insensitive to the age. If the overall age scale is uncertain at the 1σ level of individual cluster ages (50–120 Myr), we would have $\langle M_V \rangle$ = –3.90 and –3.96 mag for 10-day period Cepheids at 50 and 120 Myr, respectively.

We estimated the error from the reddening laws using different prescriptions for the color-dependent $E(B-V)$ and R_V in Feast & Walker (1987) and Laney & Stobie (1993). For the same $E(B-V)_0$ and $R_{V,0}$ values derived from the cluster MS fitting, we found that these prescriptions result in a fainter *P-L* relation by $\Delta\langle M_V \rangle \approx 0.05$ than our default case (eqs. [2] and [3]).

The average $R_{V,0}$ that we inferred from the clusters in this study is 3.19 (Table 9), which is in good agreement with the average Galactic value for the diffuse interstellar medium, $R_V \sim 3.1$. The formal standard deviation of $R_{V,0}$ is 0.17, but individual errors are too large to detect a cluster-to-cluster variation. Even if we adopt a different $R_{V,0}$, it would have a reduced impact on $\langle M_V \rangle$. This is because a larger R_V makes an MS-fitting distance shorter (Paper III), but it makes the extinction correction larger at the same time (eq. [10]).

In § 5.1 we considered the case where the presence of differential reddening makes it difficult to estimate individual extinctions for Cepheids. This is independent of the MS-fitting technique in the sense that it does not affect any of the cluster parameters. However, differential reddening could also modify cluster parameters because of cluster binaries. Unresolved binaries are typically brighter and redder than a single-star MS, which would make a distance apparently shorter. If there exists differential reddening across the cluster field, the distribution of these binaries on CMDs would be modified, and the MS-fitting parameters would subsequently change.

To estimate the effect of differential reddening, we performed artificial cluster CMD tests as described earlier in § 5.1. We assumed that $E(B-V)$ has a normal distribution

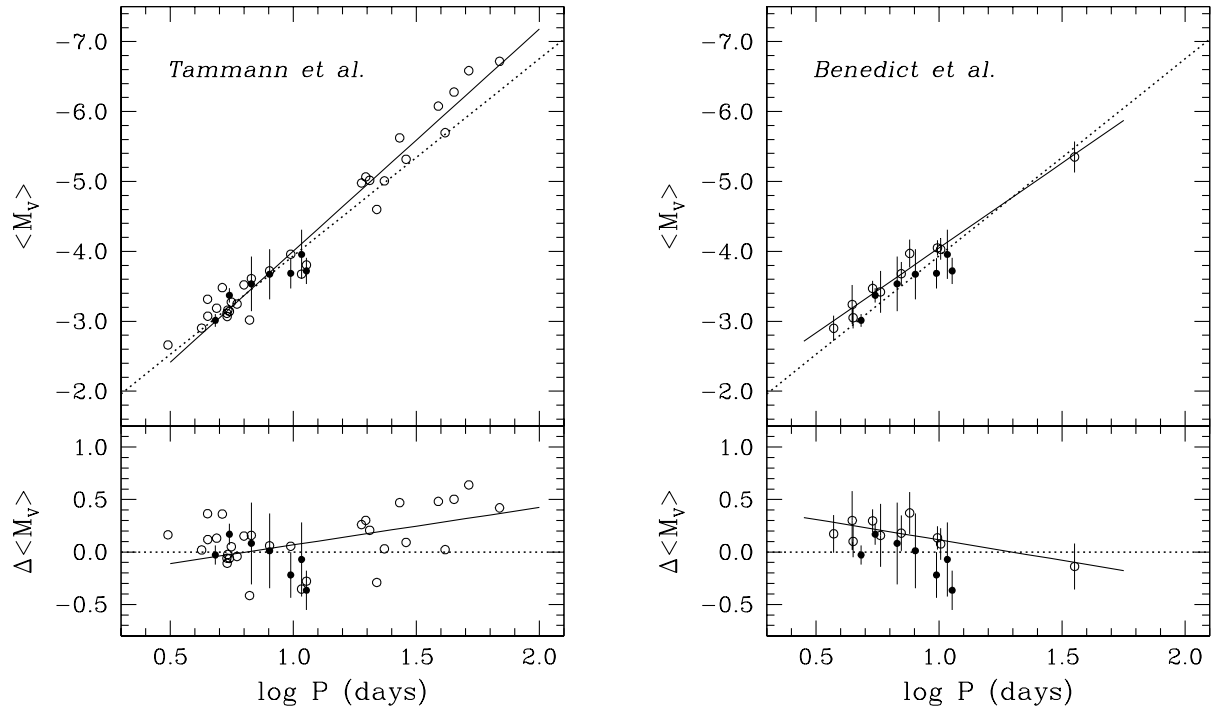


FIG. 16.— Comparison of the *V*-band Galactic *P-L* relation with those in Tammann et al. (2003, *left)* and Benedict et al. (2007, *right)*. The open circles are Cepheids in these studies, and the solid lines are their best-fit *P-L* relations. Our Galactic calibrators are shown as filled circles, and the dotted lines represent our *P-L* relation. Magnitudes in Tammann et al. were revised assuming the same Pleiades distance scale as in this paper.

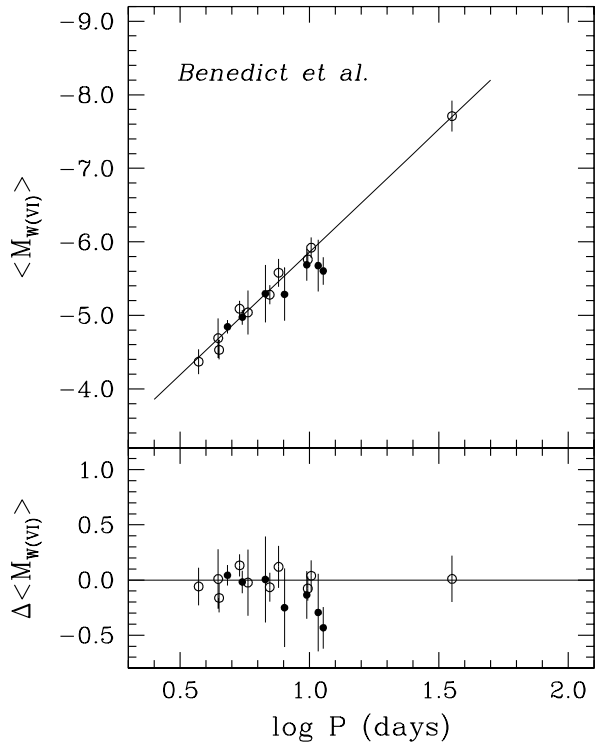


FIG. 17.— Same as Fig. 16, but a comparison of the *P-L* relation in $M_{W(VI)}$ with that of Benedict et al. (2007, *solid line)*. Residuals are shown with respect to their *P-L* relation in the bottom panel.

with a standard deviation $\sigma_{E(B-V)}$. For each set of artificial cluster CMDs we applied the photometric filtering and estimated $R_{V,0}$, $E(B-V)_0$, $(m-M)_0$, and $\langle M_V \rangle$ as for the actual cluster data, assuming $\langle B_0 \rangle - \langle V_0 \rangle = 0.7$ for Cepheids. Each panel in Figure 18 shows the bias in each of these quantities as a function of $\sigma_{E(B-V)}$. The thick solid line shows the median of the bias from 200 artificial cluster CMDs, and each set of CMDs contained 60 single stars and 40 unresolved binaries in our MS-fitting range for the distance determination. Thin lines on either side are the first and third quartiles of these estimates. The dashed line indicates a zero bias.

Even in the presence of a small differential reddening, low mass-ratio binaries cannot be easily detected from the photometric filtering. Because these unresolved binaries are redder than a single-star MS at a given M_V, the reddening would be overestimated as shown in Figure 18 for $\sigma_{E(B-V)} \lesssim 0.05$. A higher $E(B-V)$ then results in a longer distance, and a Cepheid would look brighter by several hundredths of a magnitude in $\langle M_V \rangle$. As differential reddening becomes stronger, binaries would be more scattered around the MS, and it would become further difficult to distinguish them from highly reddened single stars. As a result, both cluster reddening and distance estimates decrease at $\sigma_{E(B-V)} \gtrsim 0.05$, while semi-interquartile ranges continuously increase. We also experimented with 30% and 50% binary fractions but found insignificant changes within the semi-interquartile ranges.

The last column in Table 14 shows the size of the bias in $\langle M_V \rangle$ for each Cepheid, which was determined at $\sigma_{E(B-V)}$ in the second column. Applying these corrections to $\langle M_V \rangle$ in Table 12 leads to 0.05 mag reduction in $\langle M_V \rangle$ for 10-day period Cepheids, again making worse the agreement with the brighter calibration in the previous studies. The total χ^2 of the fit becomes smaller (6.9 for 6 degrees of freedom) if we add in quadrature the semi-interquartile range to the error in $\langle M_V \rangle$.

In summary, our Galactic *P-L* relation in *V*-band has a statistical error of 0.07 mag and a systematic error of 0.14 mag in the zero point (Table 16). If we add these quantities in quadra-

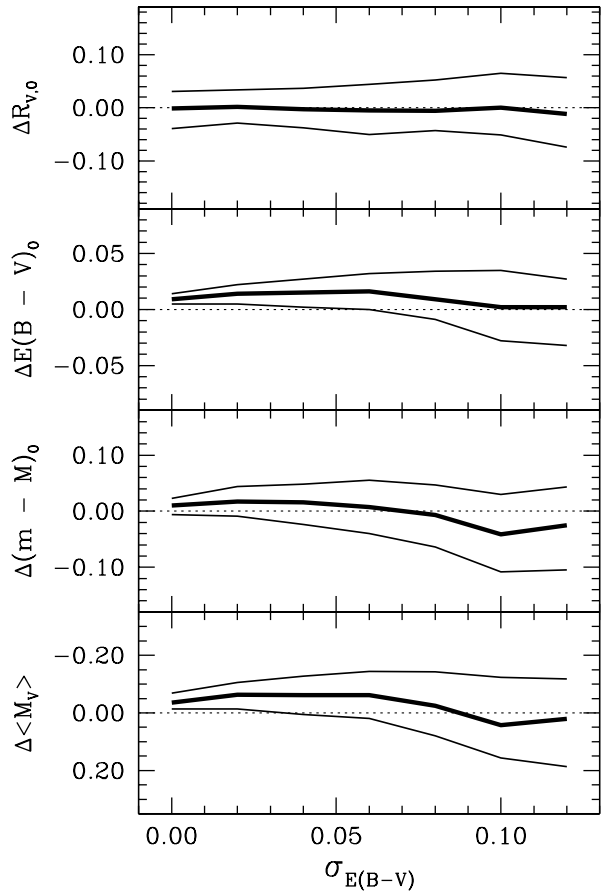


FIG. 18.— Effects of differential reddening from artificial cluster CMD tests (see text for details). A bias in each quantity is shown assuming 40% binary fraction. The thick solid line is the median of these values from 200 artificial cluster CMDs as a function of differential reddening, and thin lines on either side are the first and third quartiles. The dashed line indicates a zero bias. The differences are in the sense that Cepheids look brighter at $\sigma_{E(B-V)} \approx 0.05$ with an overestimation of $E(B-V)$.

ture, the combined error would be 0.16 mag. Since we determined the Galactic *P-L* relations in other filter passbands with the same cluster distance, reddening, and R_V estimates as in V, their zero-point errors are correlated with each other. Therefore, we took 0.16 mag as a systematic error in the Cepheid distance scale in the following section.

6. EXTRAGALACTIC DISTANCE SCALES

Cepheids have long served as our most commonly used standard candles for extragalactic distance studies. The conventional way of estimating extragalactic Cepheid distances is to use a fiducial *P-L* relation derived from the LMC Cepheids with an adopted distance to the LMC. However, geometric distances to a few galaxies have become available in recent years, providing an opportunity to compare with the Cepheid distance scale. In this section we therefore apply our Galactic *P-L* relations to estimate a distance to NGC 4258 (M106) that has an accurate geometric distance measurement from its water maser sources (Herrnstein et al. 1999). We then infer a distance to the LMC and compare our result with those adopted by the *HST* Key Project and the SN Ia calibration program (Sandage et al. 2006), from which we consider a possible increase in their Hubble constant H_0 measurements. We finish with a discussion of the potentially interesting case of M33 (NGC 598). Our most fundamental conclusion is that the distance to NGC 4258 is in good agreement with the geometric measurement when using the *P-L* relations inferred from open clusters. We also compare our LMC distance with those from the *HST* (Benedict et al. 2007) and the *Hipparcos* parallax studies (van Leeuwen et al. 2007).

TABLE 17
DISTANCE MODULUS AND METALLICITY SENSITIVITY IN NGC4258

Filter	$(m-M)_0$		γ
	Inner Field	Outer Field	mag dex^{-1}
B	29.25 ± 0.05	29.33 ± 0.07	–0.20
V	29.26 ± 0.04	29.32 ± 0.05	–0.16
I_C	29.26 ± 0.03	29.32 ± 0.04	–0.17
Average	29.26 ± 0.02	29.32 ± 0.03	–0.17

NOTE. — Distances are shown at the best-fit reddening from the Galactic *P-L* relations (see text). Errors represent fitting uncertainties, and do not include the error from the correlation with reddening.

6.1. *The Maser-host Galaxy NGC 4258*

Herrnstein et al. (1999) inferred a geometric distance to NGC 4258 from the orbital motions of water maser sources on its nucleus and found $(m-M)_0 = 29.29 \pm 0.09$ (statistical) $\pm$ 0.12 (systematic) (see also Argon et al. 2007). Many Cepheids were also observed in this galaxy, providing an opportunity to check the Cepheid distance scale (Maoz et al. 1999; Newman et al. 2001). Recently, Macri et al. (2006) discovered 281 Cepheids and provided accurate *BVI* photometry using the Advanced Camera for Surveys/Wide Field Camera (ACS/WFC) onboard the *HST*. In particular, they observed two fields in the galaxy, located at two different galactocentric distances with significantly different gas-phase metal abundances, and derived the metallicity sensitivity of the Cepheid luminosity.

We reexamined the Macri et al. data set in light of our revised *P-L* relationship. Following their selection procedure, we used the "restricted" sample of 69 Cepheids and estimated distance moduli for the two groups of Cepheids in the inner (with a period cut of $P > 12$ days) and outer fields ($P > 6$ days). For each group of this sample we corrected for extinction using our *P-L* relations in BVI_C. The absolute distance to NGC 4258 was then estimated by anchoring our Galactic sample to a reference gas-phase metal abundance within the galaxy.

Figure 19 shows how we determined the average distance and reddening. In the left two panels *apparent* distance moduli in BVI_C are shown for Cepheids in the inner and outer fields (*top* and *bottom*, respectively). Distances from shorter wavelength filters are systematically longer, and the data are well fitted by a CCM89 extinction curve (*solid line*). Here we assumed $R_V = 3.35$ for the Cepheids, which was computed from the average $R_{V,0}$ of our cluster sample with equation (2) at $\langle B\rangle_0 - \langle V\rangle_0 = 0.72$. At this value, the CCM89 extinction law yields absorption ratios A_λ/A_V of 1.30 and 0.61 for B and I_C, respectively, where we took effective wavelengths of these filters from BCP98. We added 0.02 mag in quadrature to the fitting error to take into account the photometric zero-point error. At the limit of $\lambda^{-1} \to 0$, an intercept on the ordinate is the true or unreddened distance modulus (e.g., Madore & Freedman 1991, 1998). The right two panels in Figure 19 show likelihood contours in the average reddening and dis-

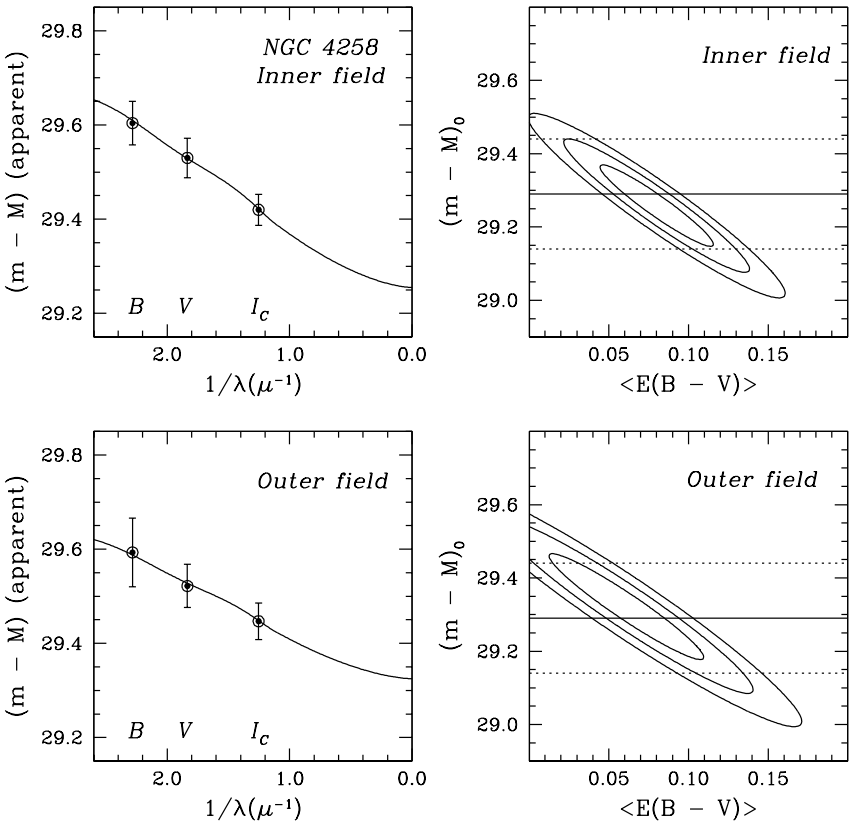


FIG. 19.— *Top left*: Apparent distance moduli of inner field Cepheids in NGC 4258 with the best-fitting CCM89 extinction curve (*solid line*). *Top right*: Likelihood contours in the average reddening and distance modulus of inner field Cepheids shown at $\Delta\chi^2$ = 2.30, 6.17, and 11.8 (68.3%, 95.4%, and 99.73% confidence levels for 2 degrees of freedom). The horizontal lines represent a geometric distance from the water maser sources and its 1σ error (Herrnstein et al. 1999). *Bottom left*: Same as the top left panel, but for outer field Cepheids. *Bottom right*: Same as the top right panel, but for outer field Cepheids.

tance modulus from these fits. Contours are shown at $\Delta\chi^2$ = 2.30, 6.17, and 11.8 (68.3%, 95.4%, and 99.73% confidence levels) for 2 degrees of freedom. Horizontal lines represent the distance estimate from the water maser sources and its combined 1σ error (Herrnstein et al. 1999). Distance moduli at the best-fit reddening are listed in Table 17 for each of the two galactic fields.

When the reddening is constrained in this way, distances in both fields are in good agreement with the maser distance. However, the distance from the inner field is shorter than the distance from the outer field by $\Delta(m-M)_0 = 0.07$. The most natural interpretation of this difference is that it measures the metallicity dependence of the Cepheid luminosity. This effect has been extensively discussed in the literature and tested empirically (Freedman & Madore 1990; Gould 1994; Sasselov et al. 1997; Kochanek 1997; Kennicutt et al. 1998; Udalski 2000; Kennicutt et al. 2003; Groenewegen et al. 2004; Sakai et al. 2004; Storm et al. 2004; Romaniello et al. 2005; Macri et al. 2006).

To estimate the true distance modulus of the galaxy, we first estimated metal abundances in the two NGC 4258 fields and then inferred a distance at the metallicity of the Galactic Cepheids. Stellar abundances cannot be measured directly for most of the Cepheid galaxies. Instead, the *HST* Key Project adopted "empirical" gas-phase [O/H] abundances from Zaritsky et al. (1994). Macri et al. computed oxygen abundances at each Cepheid's location from the H II region abundance gradient in Zaritsky et al.. The average abundances from this table are $\langle 12+\log(\mathrm{O/H})\rangle$ = 8.94 and 8.54 dex for the inner and outer field Cepheids, respectively, when the LMC Cepheids have $12+\log(\mathrm{O/H}) = 8.50$ on this scale (Sakai et al. 2004). To relate these abundances to those of our Galactic Cepheid sample, we adopted a stellar abundance difference between the LMC Cepheids and Galactic supergiants from Luck et al. (1998) of $\Delta\langle[\mathrm{Fe/H}]\rangle(\mathrm{Galaxy}-\mathrm{LMC}) \approx 0.30$. They also found a similar α-element enhancement between the LMC and the Galactic samples. In the following discussion we adopted $\Delta\langle\log(\mathrm{O/H})\rangle(\mathrm{Galaxy}-\mathrm{LMC}) = 0.30 \pm 0.06$, assuming that the stellar abundance difference is the same as the difference in the gas-phase oxygen abundance.

Since the metallicity of the Galactic Cepheids is found between the metal abundances for the inner and outer fields, the true distance would lie between distance estimates from the two galactic fields. From a linear interpolation, we obtained $(m-M)_0 = 29.28 \pm 0.10 \pm 0.16$ (*P*-*L* zero point) for a distance to NGC 4258, which is in good agreement with the current maser distance. The first error is from the fit to the *HST* ACS data (0.10 mag), an error in R_V (∓ 0.03 mag for ± 0.5 change in R_V), and an error in the metallicity scale (∓ 0.02 mag for ± 0.10 dex). We adopted an error in the metallicity scale of ± 0.10 dex to account for a possible difference in the stellar and gas-phase abundances, but it has only a moderate effect on the distance determination.

Previous studies found somewhat longer Cepheid distances to NGC 4258 although these values are consistent within the errors with the maser solution. As a part of the *HST* Key Project, Maoz et al. (1999) estimated $(m-M)_0 = 29.54 \pm 0.12 \pm 0.18$ using the Wide-Field Planetary Camera 2 (WFPC2), and Newman et al. (2001) revised it to be $(m-M)_0 = 29.47 \pm 0.09 \pm 0.15$, where the first errors repre-

sent those unique to each determination and the second errors are systematic uncertainties in the *HST* Key Project distances.

However, the reddening in the *HST* Key Project is significantly larger than our estimates. The final result in the *HST* Key Project lists $\langle E(V-I)_C\rangle = 0.22 \pm 0.04$ or $\langle E(B-V)\rangle = 0.17 \pm 0.03$ for Cepheids located in the middle of galactocentric distances to the two ACS fields. On the other hand, we found $\langle E(B-V)\rangle = 0.08 \pm 0.04$ and 0.06 ± 0.05 for the inner- and outer-field Cepheids, respectively, where the errors are the 1σ contour sizes in Figure 19. Macri et al. also estimated individual Cepheid reddenings using the OGLE-II LMC *P-L* relations, and their average values are also larger than ours, being $\langle E(B-V)\rangle = 0.18$ and 0.13 mag for the inner and outer fields, respectively.

In Table 17 we also listed the metallicity sensitivity (γ) in each band, which was computed from the distances and the average abundance difference in the two galactic fields. The magnitude of this effect is smaller than the original estimate in Macri et al., $\gamma = -0.29 \pm 0.09$ (random) ± 0.05 (systematic) mag dex^{-1}. Since our estimate neglects the change in color with metallicity, we employed the metallicity corrections from Kochanek (1997) in the next two sections. Kochanek derived corrections in *UBVRIJHK* based on a simultaneous analysis of Cepheids in 17 galaxies with a proper treatment of correlations between extinction, temperature, and metallicity. The corrections are $+0.20 \pm 0.18$, -0.08 ± 0.14, -0.21 ± 0.14, -0.26 ± 0.13, -0.34 ± 0.14, and -0.40 ± 0.13 mag dex^{-1} in BVI_CJHK, respectively, in the sense that metal-rich Cepheids have a decreased flux in *B* but increased fluxes in VI_CJHK, possibly due to line-blanketing and back-warming among other effects. These estimates are based on $\langle E(B-V)\rangle = 0.15$ for LMC Cepheids, but their dependence on the LMC reddening is small. If we adopt these corrections for NGC 4258, we would derive $(m-M)_0 = 29.34 \pm 0.13$ for the inner-field and 29.17 ± 0.19 mag for the outer-field Cepheids, where the errors represent the 1σ statistical uncertainty.

6.2. *LMC*

Our Galactic *P-L* relations can also be applied to estimate the distance to the LMC and its mean reddening. We included JHK_s photometry of the LMC Cepheids from Persson et al. (2004), as well as BVI_C photometry from the OGLE-II catalog in the multi-wavelength fitting technique. This approach assumes that Cepheids in these two surveys were drawn from the same population.[10]

Figure 20 shows likelihood contours in the solution for the average LMC reddening and its distance modulus (*middle panel*) from the fits on the apparent distance moduli in BVI_CJHK_s (*left panel*). We applied metallicity corrections for $\Delta\langle\log(\mathrm{O/H})\rangle(\mathrm{Galaxy}-\mathrm{LMC}) = 0.30$ and assumed that the metallicity sensitivities on the Glass-Carter *JHK* system in Kochanek (1997) are the same as in the LCO JHK_s system. As in the NGC 4258 case, we assumed $R_V = 3.35$ for the Cepheids, which yields absorption ratios A_λ/A_V of 0.29, 0.18, and 0.12 for JHK_s, respectively, from the CCM89 extinction law. In this calculation we took the effective filter wavelengths from Persson et al. (2004) for JHK_s on the LCO system. We added 0.02 mag in BVI_C (Udalski et al. 1999a) and 0.03 mag in JHK_s (Persson et al. 2004) in quadrature to the fitting errors to account for photometric zero-point errors.

[10] The OGLE-II Cepheids were observed along the LMC bar, while the Cepheids observed in JHK_s (Persson et al. 2004) are more dispersed over the LMC.

TABLE 18
DISTANCE MODULUS OF THE LMC

Filter	$(m-M)_0$	
	OGLE-II $E(B-V)$[a]	Best-fit $E(B-V)$[b]
B	18.19 ± 0.06	18.35 ± 0.06
V	18.23 ± 0.05	18.34 ± 0.05
I_C	18.29 ± 0.05	18.35 ± 0.05
J	···	18.35 ± 0.05
H	···	18.32 ± 0.05
K_s	···	18.36 ± 0.05
Average	18.24 ± 0.03	18.34 ± 0.02

NOTE. — After applying metallicity corrections from Kochanek (1997).

[a] Distances derived assuming the OGLE-II reddening map.

[b] Distances shown at the best-fit reddening from the Galactic *P-L* relations (see text). Errors represent fitting uncertainties, and do not include the error from the correlation with reddening.

As shown in Figure 20, our best-fit solution yields $(m-M)_0 = 18.34 \pm 0.06 \pm 0.16$ (*P-L* zero point). Extinction-corrected distance moduli at the best-fit reddening are listed in Table 18. The first error in distance is a quadrature sum of a fitting error (± 0.05 mag) and an error from R_V (∓ 0.01 mag for ± 0.5 in R_V). We also added in quadrature an error from the metallicity (∓ 0.03 mag for ± 0.06 dex). As in the NGC 4258 case the zero-point error of the Galactic *P-L* relations dominates the combined error in the LMC distance modulus. Without metallicity corrections, we would derive $(m-M)_0 = 18.48$.

We also derived $\langle E(B-V)\rangle = 0.11 \pm 0.02$, where the error is from the 1σ contour in Figure 20. Our average reddening is 0.03 mag smaller than the average reddening from the OGLE-II, $\langle E(B-V)\rangle = 0.143$, which was adopted in the *HST* Key Project.[11] However, our reddening estimate is closer to the value of $E(B-V) \sim 0.10$ (Walker 1999) from several different reddening estimates for LMC stars (see Table II in McNamara & Feltz 1980). It is also in agreement with the reddening value determined for the LMC Cepheids, $\langle E(B-V)\rangle = 0.076$ (Caldwell & Coulson 1985; Laney & Caldwell 2007). The zero point of the OGLE-II reddening map was set by two LMC clusters (NGC 1850 and NGC 1835) and one eclipsing binary (HV 2274), but the reddening for HV 2274 has different values from various studies: OGLE-II adopted $E(B-V) = 0.149 \pm 0.015$ (Udalski et al. 1998), which is larger than $E(B-V) = 0.120 \pm 0.009$ (Guinan et al. 1998), 0.088 ± 0.023 (Nelson et al. 2000), and 0.103 ± 0.007 (Groenewegen & Salaris 2001). Furthermore, as shown in Table 18, extinction corrections from the OGLE-II reddening map result in systematically shorter distances at shorter wavelengths, which may indicate an overcorrection for extinction (see also Fouqué et al. 2003).

Our distance modulus is 0.16 mag smaller (or 7% in distance) than the adopted distance modulus by the *HST* Key Project (18.50 mag). Formally, this implies an increase in their H_0 by $7\% \pm 8\%$. Our LMC distance is also shorter by 0.20 mag (or 9% in distance) than the distance modulus adopted by the Sandage et al. (2006) program (18.54 mag). In addition to our study, recent parallax studies from the *HST* (Benedict et al. 2007) and the revised *Hipparcos* catalog (van Leeuwen et al. 2007) used the Wesenheit index W_{VI} to derive

[11] The *HST* Key Project adopted the OGLE-II LMC *P-L* relations and scaled them to $(m-M)_0 = 18.50$. However, the *P-L* relations were not scaled to $\langle E(B-V)\rangle = 0.10$ as they claimed (see also Fouqué et al. 2003).

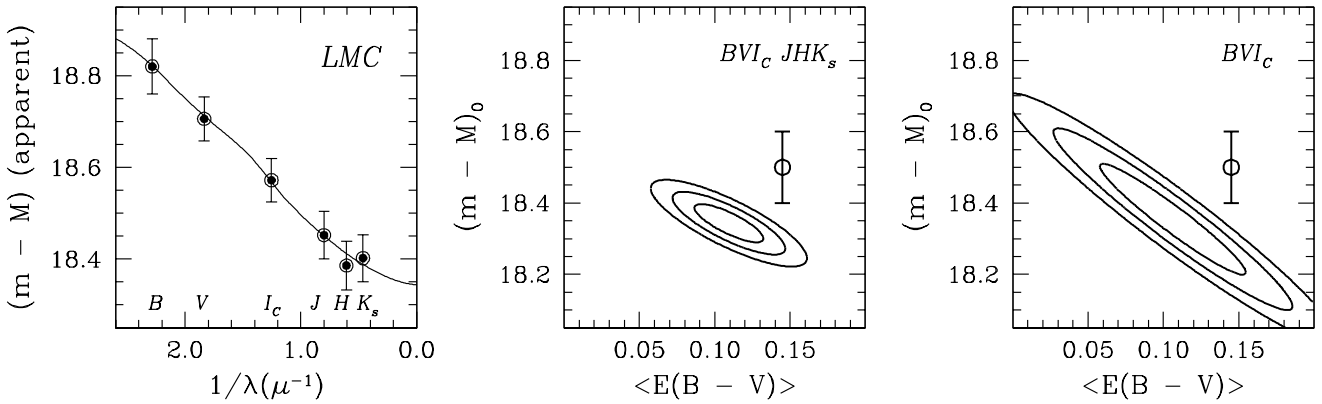


FIG. 20.— *Left*: Apparent LMC distance moduli in BVI_CJHK_s with the best-fitting CCM89 extinction curve (*solid line*). *Middle*: Likelihood contours in the average LMC reddening and its distance modulus in BVI_CJHK_s shown at $\Delta\chi^2$ = 2.30, 6.17, and 11.8 (68.3%, 95.4%, and 99.73% confidence levels for 2 degrees of freedom). The error bar represents the adopted distance and its error by *HST* Key Project at the average reddening from the OGLE-II reddening map. *Right*: Same as the left panel, but likelihood contours when BVI_C photometry is used only.

$(m-M)_0 = 18.40 \pm 0.05$ and 18.39 ± 0.05 mag, respectively, also suggesting a downward revision of the LMC distance. Finally, Macri et al. (2006) estimated a distance modulus of NGC 4258 relative to the LMC of 10.88 ± 0.04 (statistical) $\pm$ 0.05 (systematic). Given the maser distance, this was then translated into the LMC distance modulus of $(m-M)_0 = 18.41 \pm 0.10$ (statistical) ± 0.13 (systematic), which is within 1σ of our estimate.

We note that stronger constraints on distance can be achieved when several photometric bands are used including near-infrared data. As illustrated in Figure 20, the statistical error in distance becomes larger by a factor of 3 when only BVI_C information is used (*right panel*) rather than from BVI_CJHK_s (*middle panel*). The error would be even larger when the distance and reddening values are estimated from only two bands, such as the Wesenheit index.

6.3. *M33*

As our final case, we estimated the average distance and reddening for M33 Cepheids using the same method as in the previous section. The distance to this nearby spiral galaxy has recently been measured from a detached eclipsing binary, $(m-M)_0 = 24.92 \pm 0.12$ (Bonanos et al. 2006), and from two water maser sources in H II regions, $(m-M)_0 = 24.32^{+0.45}_{-0.57}$ (Brunthaler et al. 2005).

Figure 21 shows likelihood contours in the solution for the average reddening and distance modulus. As in the *HST* Key Project, we used BVI_C photometry in Freedman et al. (1991) for their 10 best observed Cepheids, which was obtained at the 3.6 m Canada-France-Hawaii Telescope (CFHT), the Kitt Peak National Observatory (KPNO) 4 m telescope, and the Palomar 1.5 m telescope. We assumed 0.03 mag for the photometric zero-point error in each band. On the Zaritsky et al. (1994) scale, M33 Cepheids have $\langle 12 + \log(\mathrm{O/H})\rangle = 8.82$, which was adopted in the *HST* Key Project. We therefore applied metallicity corrections from Kochanek (1997) for $\Delta\langle\log(\mathrm{O/H})\rangle(\mathrm{Galaxy}-\mathrm{M33}) = -0.02$.

At the best-fit reddening, we obtained an extinction-corrected distance modulus of 24.51 ± 0.11, 24.60 ± 0.09, and 24.53 ± 0.08 in BVI_C, respectively, where the uncertainties are fitting errors only. The average distance is $(m-M)_0 = 24.55 \pm 0.28 \pm 0.16$ (*P-L* zero point). The first error was determined by adding in quadrature the fitting error (0.28 mag), the error from R_V (∓ 0.03 mag for $\Delta R_V = \pm 0.5$), and the error from the metallicity (∓ 0.08 mag for ± 0.15 dex). We adopted the error in the metallicity from the *HST* Key Project. If we adopt metal abundances derived from electron temperatures (Sakai et al. 2004), the abundance difference between the LMC and M33 becomes $\Delta\langle\log(\mathrm{O/H})\rangle = +0.21$, which leads to $\Delta\langle\log(\mathrm{O/H})\rangle(\mathrm{Galaxy}-\mathrm{M33}) = +0.09$. We would derive $(m-M)_0 = 24.53$ without metallicity corrections.

The HST Key Project used the same ground-based photometry for this galaxy and derived a metallicity-corrected distance modulus of $(m-M)_0 = 24.62 \pm 0.15$ based only on *VI* as for the other *HST* sample galaxies. While this distance is in good agreement with our estimate, our average reddening of $\langle E(B-V)\rangle = 0.08 \pm 0.09$ is lower than their estimate, $\langle E(V-I)\rangle = 0.27 \pm 0.05$ or $\langle E(B-V)\rangle = 0.21 \pm 0.04$.[12] A part of the difference is due to different zero points of *P-L* relations. However, our reddening is in good agreement with the value of the eclipsing binary, $E(B-V) = 0.09 \pm 0.01$, which was obtained from $BVRJHK_s$ photometry (Bonanos et al. 2006) and with previous estimates based on several different methods (see Table 7 of Bonanos et al.).

A similar result was obtained from a larger Cepheid sample in Macri et al. (2001a). They provided BVI_C photometry for 251 Cepheids obtained at the Fred Lawrence Whipple Observatory (FLWO) 1.2 m telescope and the MDM 1.3 m telescope (see also Mochejska et al. 2001a,b). From the restricted sample of 90 Cepheids in $1.1 \leq \log P \leq 1.7$ similar to those of the Freedman et al. sample, we derived $(m-M)_0 = 24.67 \pm 0.18$ and $\langle E(B-V)\rangle = 0.04 \pm 0.06$, where the uncertainties are fitting errors only.

Distances from these two independent sets of photometry are about 0.3 mag shorter than the distance from the eclipsing binary, although our distance has a large error. One potential explanation for the short Cepheid-based distance is the unresolved blends by a strong star-to-star correlation function. Mochejska et al. (2001c) investigated the influence of blending by comparing *HST* WFPC2 and Macri et al. ground-based images for a sample of 102 Cepheids (see also Mochejska et al. 2000). They found that the average flux contribution from unresolved luminous companions on the ground-based images could be on average $\sim 20\%$ in *BVI* for $\log P > 1$, which would systematically underestimate the Cepheid distance by $\sim 10\%$. In addition, Lee et al. (2002) obtained single-epoch

[12] We note that Freedman et al. (1991) originally derived $\langle E(B-V)\rangle = 0.10 \pm 0.09$ and $(m-M)_0 = 24.64 \pm 0.09$ using *BVRI* photometry, assuming the LMC distance modulus of 18.5 mag and its mean reddening of 0.10 mag.

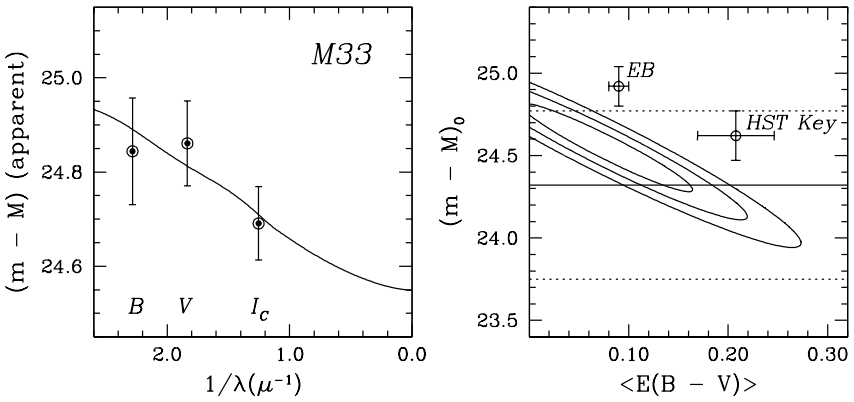


FIG. 21.— *Left:* Apparent distance moduli in BVI_C with the best-fitting CCM89 extinction curve (*solid line*). *Right:* Likelihood contours in the average reddening and distance modulus of M33 Cepheids shown at $\Delta\chi^2$ = 2.30, 6.17, and 11.8 (68.3%, 95.4%, and 99.73% confidence levels for 2 degrees of freedom). Two open circles represent the distance and reddening estimates from an eclipsing binary (Bonanos et al. 2006) and those from the *HST* Key Project. The horizontal lines represent a distance from the water maser sources and its 1σ error (Brunthaler et al. 2005).

I-band photometry for a subset of the Macri et al. sample using *HST* WFPC2 and found that the *HST* photometry is on average ≈ 0.2 mag fainter than Macri et al. photometry.

Follow-up observations with a higher spatial resolution (e.g., Macri 2004) would be helpful for a definitive test of the distance to M33, although there are indications that our estimated reddening is more accurate than the value in the *HST* Key Project. Note that the effect of stellar blending is less significant in our distance estimates for NGC 4258 and the LMC. The ground-based photometry with the full width at half-maximum (FWHM) of $\sim 1.5''$ would correspond to ~ 0.3 pc at the distance of the LMC, compared to ~ 7 pc at the distance of M33. The ACS/WFC FWHM of $0.09''$(Ford et al. 2003) corresponds to ~ 3 pc at the distance of NGC 4258.

7. SUMMARY AND DISCUSSION

We have continued our effort to improve the accuracy of isochrones and distances derived from MS fitting. We extended the previous Hyades-based calibration to the upper MS by constructing empirical color-$T_{\rm eff}$ corrections to match the observed Pleiades MS at the cluster's accurately known distance. We applied these empirically calibrated sets of isochrones to Cepheid-bearing Galactic open clusters to derive distances, reddenings, and R_V at the spectroscopic metal abundances and obtained Galactic *P-L* relations based on nine Cepheids in seven clusters. Our distance modulus of individual Cepheids has an accuracy of ~ 0.08 mag (or 4% in distance), which is compatible to those of recent parallaxes from the *HST* (Benedict et al. 2007) and the revised *Hipparcos* catalog (van Leeuwen et al. 2007).

Using these *P-L* relations, we derived a distance to NGC 4258 and found that our Cepheid distance is in excellent agreement with the maser distance, supporting our distance scale from the MS-fitting technique. From BVI_CJHK_s photometry we derived the LMC distance modulus of $(m-M)_0 = 18.34 \pm 0.06 \pm 0.16$ (*P-L* zero point) after applying metallicity corrections. This is also in close agreement with distance estimates from the recent *HST* and *Hipparcos* parallax studies. However, our revised LMC distance is lower than the distance adopted by the *HST* Key Project, which formally implies an increase in their H_0 by $7\% \pm 8\%$. A similar size of an increase in H_0 is expected from the SN Ia calibration program by Sandage et al. (2006).

Our reddening estimates are systematically lower than those in the *HST* Key Project. Part of the reason is the *P-L* relations with different assumptions about the reddening. They adopted the color excess for LMC Cepheids from the OGLE-II reddening map, but its average value is $\Delta\langle E(B-V)\rangle \approx 0.03$ larger than our LMC reddening estimate. Nonetheless, relative distances between the LMC and target galaxies in the *HST* Key Project would remain less affected because the reddening-free or Wesenheit index adopted in the *HST* Key Project is designed to avoid the problem of knowing the absolute zero point of the reddening scale. In other words, the absolute reddening value would not be important as long as the difference in reddening between target Cepheids and the calibrating system is well-defined. Therefore, the Wesenheit index can be effectively used to build the cosmic distance scale once highly accurate distances to calibrating Cepheids are available.

However, our $E(B-V)$ estimates for NGC 4258 and M33 are larger by $\langle E(B-V)\rangle \sim 0.1$ than those in the *HST* Key Project, more than expected from the difference in the LMC reddening. This is due to two reasons. First, the Cepheid's color is not only affected by reddening, but it can be also affected by the metal content. The *HST* Key Project corrected a distance modulus for a metallicity effect after deriving a color excess. On the other hand, we applied metallicity corrections to apparent distance moduli from Kochanek (1997), and then derived a reddening value. Because the sign and size of the metallicity corrections could not be the same in different broadband filters, the difference in the Cepheid metallicity could lead to different reddening estimates from those in the *HST* Key Project. Second, the Wesenheit magnitude is based on only two broadband filters. However, reddening and distance estimates are naturally correlated in the standard procedure to estimate these parameters using *P-L* relations, so a small zero-point error in the photometry, for example, can be translated into a large error in reddening. Therefore, obtaining Cepheid photometry at least in three or more passbands including near-infrared filters is of great importance in the distance and reddening estimation (e.g., Gieren et al. 2006; Soszyński et al. 2006).

In the determination of individual Cepheids' absolute magnitudes, the extinction is one of the largest sources of error because of strong differential reddening in Cepheid-bearing young open clusters. Although we found an error of ~ 0.03 mag in the mean $E(B-V)$ for a cluster, most Cepheid-bearing clusters have patchy reddening that makes the individ-

ual Cepheid reddening uncertain by up to $\sigma_{E(B-V)} \sim 0.12$. An average reddening of cluster members located near a Cepheid was often used to determine the Cepheid's reddening, but differential reddening over a small scale could not be resolved unless we have a sufficient number of nearby stars with well-determined reddening. However, it is noted that the most secure reddening estimates for Cepheids are considered to be given by the cluster Cepheids. In addition, our LMC reddening is in close agreement with the previous standard value, $\langle E(B-V)\rangle \sim 0.10$ (Walker 1999), and our average reddening for M33 Cepheids is in good agreement with the value inferred from $BVRJHK_s$ photometry of an eclipsing binary (Bonanos et al. 2006).

In terms of the zero point of the Galactic *P-L* relations, the uncertainty in the metallicity scale of the Galactic open clusters is the largest error source, with a change of Δ[M/H] $\sim$ 0.1 dex producing a ~ 0.1 mag shift in distance modulus. No other source is unusually large. In Paper III we have shown that several color indices can be effectively used in MS fitting to determine a cluster metallicity because of differential sensitivities of these colors on metal abundance. Although the noise in the current photometry prevented the estimation of the photometric metal abundance, deep multi-color photometry combined with near-infrared data will be useful to determine R_V, $E(B-V)$, $(m-M)_0$, and [M/H], simultaneously. A more accurate metallicity scale could then be used to reduce the size of the systematic error in the *P-L* zero point. In addition, the zero-point error can be further reduced by deeper photometry of other Cepheid-bearing clusters, which were not included in this paper because of poor photometric quality. These are C1814-191, Collinder 394, Mon OB2, NGC 1647, NGC 6649, NGC 6664, Platais 1, Trumpler 35, Vel OB5, and Vul OB1.

We are very grateful to Krzysztof Stanek for his valuable comments and suggestions. We gratefully acknowledge Michael Bessell for answering a number of questions about his computations of color-excess ratios, Fiona Hoyle for providing her photometry, and Imants Platais for pointing out some problematic features of the isochrones, which has led us to investigate the LCB color correction tables more carefully. We also would like to thank Andrew Gould, Lucas Macri, Fritz Benedict, Christopher Kochanek, and Jennifer Johnson for useful discussions. We thank Richard Pogge, Subo Dong, and Kristen Sellgren for their help. The work reported here was partially supported by grants AST-0206008 and AST-0205789 from the National Science Foundation to the Ohio State Research Foundation, and with funds provided by the Ohio State University Department of Astronomy. This publication makes use of data products from the Two Micron All Sky Survey, which is a joint project of the University of Massachusetts and the Infrared Processing and Analysis Center/California Institute of Technology, funded by the National Aeronautics and Space Administration and the National Science Foundation.

REFERENCES

Allen, C. W. 1973, Astrophysical Quantities (London: Athlone)
Alonso, A., Arribas, S., & Martínez-Roger, C. 1995, A&A, 297, 197
Alonso, A., Arribas, S., & Martínez-Roger, C. 1996, A&AS, 117, 227
An, D., Terndrup, D. M., Pinsonneault, M. H., Paulson, D. B., Hanson, R. B., & Stauffer, J. R. 2007, ApJ, 655, 233 (Paper III)
Andrievsky, S. M., et al. 2002, A&A, 381, 32
Argon, A. L., Greenhill, L. J., Reid, M. J., Moran, J. M., & Humphreys, E. M. L. 2007, ApJ, 659, 1040
Arp, H. 1960, ApJ, 131, 322
Arp, H., Sandage, A., & Stephens, C. 1959, ApJ, 130, 80
Bahcall, J. N., & Pinsonenault, M. H. 2004, Phys. Rev. Lett., 92, 121301
Bahcall, J. N., Pinsonneault, M. H., & Basu, S. 2001, ApJ, 555, 990
Basu, S., Pinsonneault, M. H., & Bahcall, J. N. 2000, ApJ, 529, 1084
Baumgardt, H., Dettbarn, C., & Wielen, R. 2000, A&AS, 146, 251
Benedict, G. F., et al. 2002a, AJ, 123, 473
Benedict, G. F., et al. 2002b, AJ, 124, 1695
Benedict, G. F., et al. 2007, AJ, 133, 1810
Berdnikov, L. N., Dambis, A. K., & Vozyakova, O. V. 2000, A&AS, 143, 211
Bessell, M. S. 2005, ARA&A, 43, 293
Bessell, M. S., Castelli, F., & Plez, B. 1998, A&A, 333, 231 (BCP98)
Böhm-Vitense, E., Evans, N. R., Carpenter, K., Albrow, M. D., Cottrell, P. L., Robinson, R., & Beck-Winchatz, B. 1998, ApJ, 505, 903
Bonanos, A. Z., et al. 2006, ApJ, 652, 313
Breger, M. 1966, PASP, 78, 293
Breger, M. 1986, ApJ, 309, 311
de Bruijne, J. H. J., Hoogerwerf, R., & de Zeeuw, P. T. 2001, A&A, 367, 111
Brunthaler, A., Reid, M. J., Falcke, H., Greenhill, L. J., & Henkel, C. 2005, Science, 307, 1440
Caldwell, J. A. R., & Coulson, I. M. 1985, MNRAS, 212, 879
Cardelli, J. A., Clayton, G. C., & Mathis, J. S. 1989, ApJ, 345, 245 (CCM89)
Carpenter, J. M. 2001, AJ, 121, 2851
Carter, B. S. 1990, MNRAS, 242, 1
Clariá, J. J., Lapasset, E., & Bosio, M. A. 1991, MNRAS, 249, 193
Cohen, M., Wheaton, W. A., & Megeath, S. T. 2003, AJ, 126, 1090
Collins, G. W., II, & Sonneborn, G. H. 1977, ApJS, 34, 41
Dean, J. F., Warren, P. R., & Cousins, A. W. J. 1978, MNRAS, 183, 569
Evans, N. R., Böhm-Vitense, E., Carpenter, K., Beck-Winchatz, B., & Robinson, R. 1997, PASP, 109, 789
Evans, N. R., Böhm-Vitense, E., Carpenter, K., Beck-Winchatz, B., & Robinson, R. 1998, ApJ, 494, 768
Evans, N. R., & Bolton, C. T. 1990, ApJ, 356, 630
Evans, N. R., Massa, D., Fullerton, A., Sonneborn, G., & Iping, R. 2006, ApJ, 647, 1387
Feast, M. W. 1957, MNRAS, 117, 193
Feast, M. 1999, PASP, 111, 775
Feast, M. 2003, in Stellar Candles for the Extragalactic Distance Scale, ed. D. Alloin & W. Gieren (Berlin: Springer), 45
Feast, M. W., & Catchpole, R. M. 1997, MNRAS, 286, L1
Feast, M., Pont, F., & Whitelock, P. 1998, MNRAS, 298, L43
Feast, M. W., & Walker, A. R. 1987, ARA&A, 25, 345
Fernie, J. D. 1961, ApJ, 133, 64
Fernie, J. D. 1990, ApJS, 72, 153
Fernie, J. D. 1994, ApJ, 429, 844
Fernie, J. D., Beattie, B., Evans, N. R., & Seager, S. 1995, IBVS No. 4148
Ford, H. C., et al. 2003, Proc. SPIE, 4854, 81
Fouqué, P., Storm, J., & Gieren, W. 2003, in Stellar Candles for the Extragalactic Distance Scale, ed. D. Alloin & W. Gieren (Berlin: Springer), 21
Freedman, W. L., & Madore, B. F. 1990, ApJ, 365, 186
Freedman, W. L., Wilson, C. D., & Madore, B. F. 1991, ApJ, 372, 455
Freedman, W. L., et al. 2001, ApJ, 553, 47
Fry, A. M., & Carney, B. W. 1997, AJ, 113, 1073
Gieren, W. P., Fouqué, P., & Gómez, M. 1997, ApJ, 488, 74
Gieren, W. P., Fouqué, P., & Gómez, M. 1998, ApJ, 496, 17
Gieren, W., Pietrzyński, G., Nalewajko, K., Soszyński, I., Bresolin, F., Kudritzki, R.-P., Minniti, D., & Romanowsky, A. 2006, ApJ, 647, 1056
Gieren, W., Storm, J., Barnes, T. G., III, Fouqué, P., Pietrzyński, G., & Kienzle, F. 2005, ApJ, 627, 224
Groenewegen, M. A. T., & Oudmaijer, R. D. 2000, A&A, 356, 849
Groenewegen, M. A. T., & Salaris, M. 2001, A&A, 366, 752
Groenewegen, M. A. T., Romaniello, M., Primas, F., & Mottini, M. 2004, A&A, 420, 655
Gould, A. 1994, ApJ, 426, 542
Guinan, E. F., et al. 1998, ApJ, 509, L21
Gupta, A. C., Subramaniam, A., Sagar, R., & Griffiths, W. K. 2000, A&AS, 145, 365
Haug, U. 1978, A&AS, 34, 417
Herrnstein, J. R., et al. 1999, Nature, 400, 539
Hertzsprung, E. 1947, Annalen van de Sterrewacht te Leiden, 19, 1
Hoag, A. A., Johnson, H. L., Iriarte, B., Mitchell, R. I., Hallam, K. L., & Sharpless, S. 1961, Publications of the U.S. Naval Observatory Second Series, 17, 345
Hoyle, F., Shanks, T., & Tanvir, N. R. 2003, MNRAS, 345, 269
Johnson, H. L. 1960, ApJ, 131, 620
Kanbur, S. M., & Ngeow, C.-C. 2004, MNRAS, 350, 962
Kennicutt, R. C., Jr., Bresolin, F., & Garnett, D. R. 2003, ApJ, 591, 801
Kennicutt, R. C., Jr., et al. 1998, ApJ, 498, 181
Kervella, P., Bersier, D., Mourard, D., Nardetto, N., & Coudé du Foresto, V. 2004a, A&A, 423, 327
Kervella, P., Nardetto, N., Bersier, D., Mourard, D., & Coudé du Foresto, V. 2004b, A&A, 416, 941
Kim, Y.-C., Demarque, P., Yi, S. K., & Alexander, D. R. 2002, ApJS, 143, 499
Kochanek, C. S. 1997, ApJ, 491, 13

Kraft, R. P. 1958, ApJ, 128, 161
Kraft, R. P. 1965, ApJ, 142, 681
Landolt, A. U. 1983, AJ, 88, 439
Landolt, A. U. 1992, AJ, 104, 340
Lane, B. F., Kuchner, M. J., Boden, A. F., Creech-Eakman, M., & Kulkarni, S. R. 2000, Nature, 407, 485
Lane, B. F., Creech-Eakman, M. J., & Nordgren, T. E. 2002, ApJ, 573, 330
Laney, C. D., & Stobie, R. S. 1992, A&AS, 93, 93
Laney, C. D., & Stobie, R. S. 1993, MNRAS, 263, 921
Laney, C. D., & Caldwell, J. A. R. 2007, MNRAS, 377, 147
Lanoix, P., Paturel, G., & Garnier, R. 1999, MNRAS, 308, 969
Lee, M. G., Kim, M., Sarajedini, A., Geisler, D., & Gieren, W. 2002, ApJ, 565, 959
Lee, J.-D., & Lee, S.-G. 1999, Journal of Korean Astronomical Society, 32, 91
Lejeune, Th., Cuisinier, F., & Buser, R. 1997, A&AS, 125, 229 (LCB)
Lejeune, Th., Cuisinier, F., & Buser, R. 1998, A&AS, 130, 65 (LCB)
Luck, R. E., Moffett, T. J., Barnes, T. G., III, & Gieren, W. P. 1998, AJ, 115, 605
Luri, X., Gómez, A. E., Torra, J., Figueras, F., & Mennessier, M. O. 1998, A&A, 335, L81
Lynga, G. 1987, Catalogue of Open Cluster Data, 5th ed. (Lund: Lund Observatory)
Macri, L. M. 2004, IAU Colloq. 193: Variable Stars in the Local Group, 310, 33
Macri, L. M., Stanek, K. Z., Bersier, D., Greenhill, L. J., & Reid, M. J. 2006, ApJ, 652, 1133
Macri, L. M., Stanek, K. Z., Sasselov, D. D., Krockenberger, M., & Kaluzny, J. 2001a, AJ, 121, 870
Macri, L. M., et al. 2001b, ApJ, 549, 721
Madore, B. F. 1975, A&A, 38, 471
Madore, B. F., & Freedman, W. L. 1991, PASP, 103, 933
Madore, B. F., & Freedman, W. L. 1998, ApJ, 492, 110
Maoz, E., Newman, J. A., Ferrarese, L., Stetson, P. B., Zepf, S. E., Davis, M., Freedman, W. L., & Madore, B. F. 1999, Nature, 401, 351
Mathis, J. S. 1990, ARA&A, 28, 37
McNamara, D. H., & Feltz, K. A., Jr. 1980, PASP, 92, 587
Mermilliod, J. C. 1981, A&A, 97, 235
Mermilliod, J. C., Mayor, M., & Burki, G. 1987, A&AS, 70, 389
Mermilliod, J.-C., & Paunzen, E. 2003, A&A, 410, 511
Meynet, G., Mermilliod, J.-C., & Maeder, A. 1993, A&AS, 98, 477
Mochejska, B. J., Kaluzny, J., Stanek, K. Z., Sasselov, D. D., & Szentgyorgyi, A. H. 2001a, AJ, 121, 2032
Mochejska, B. J., Kaluzny, J., Stanek, K. Z., Sasselov, D. D., & Szentgyorgyi, A. H. 2001b, AJ, 122, 2477
Mochejska, B. J., Macri, L. M., Sasselov, D. D., & Stanek, K. Z. 2000, AJ, 120, 810
Mochejska, B. J., Macri, L. M., Sasselov, D. D., & Stanek, K. Z. 2001c, preprint (astro-ph/0103440)
Moffat, A. F. J., & Vogt, N. 1973, A&AS, 10, 135
Moffat, A. F. J., & Vogt, N. 1975, A&AS, 20, 155
Nelson, C. A., Cook, K. H., Popowski, P., & Alves, D. R. 2000, AJ, 119, 1205
Newman, J. A., Ferrarese, L., Stetson, P. B., Maoz, E., Zepf, S. E., Davis, M., Freedman, W. L., & Madore, B. F. 2001, ApJ, 553, 562
Ngeow, C.-C., Kanbur, S. M., Nikolaev, S., Buonaccorsi, J., Cook, K. H., & Welch, D. L. 2005, MNRAS, 363, 831
Orsatti, A. M., Vega, E. I., & Marraco, H. G. 2001, A&A, 380, 130
Paulson, D. B., Sneden, C., & Cochran, W. D. 2003, AJ, 125, 3185
Perryman, M. A. C., et al. 1998, A&A, 331, 81
Persson, S. E., Madore, B. F., Krzemiński, W., Freedman, W. L., Roth, M., & Murphy, D. C. 2004, AJ, 128, 2239
Phelps, R. L., & Janes, K. A. 1994, ApJS, 90, 31
Piatti, A. E., Clariá, J. J., & Bica, E. 1998, ApJS, 116, 263
Pinsonneault, M. H., Terndrup, D. M., Hanson, R. B., & Stauffer, J. R. 2003, ApJ, 598, 588 (Paper I)
Pinsonneault, M. H., Terndrup, D. M., Hanson, R. B., & Stauffer, J. R. 2004, ApJ, 600, 946 (Paper II)
Preston, G. W. 1964, PASP, 76, 165
Ribas, I., Jordi, C., Vilardell, F., Fitzpatrick, E. L., Hilditch, R. W., & Guinan, E. F. 2005, ApJ, 635, L37
Rieke, G. H., & Lebofsky, M. J. 1985, ApJ, 288, 618
Romaniello, M., Primas, F., Mottini, M., Groenewegen, M., Bono, G., & François, P. 2005, A&A, 429, L37
Romeo, G., Bonifazi, A., Fusi Pecci, F., & Tosi, M. 1989, MNRAS, 240, 459
Sagar, R., & Cannon, R. D. 1997, A&AS, 122, 9
Sakai, S., Ferrarese, L., Kennicutt, R. C., Jr., & Saha, A. 2004, ApJ, 608, 42
Salpeter, E. E. 1955, ApJ, 121, 161
Sandage, A. 1958, ApJ, 128, 150
Sandage, A. 1960, ApJ, 131, 610
Sandage, A., & Tammann, G. A. 2006, ARA&A, 44, 93
Sandage, A., Tammann, G. A., & Reindl, B. 2004, A&A, 424, 43
Sandage, A., Tammann, G. A., Saha, A., Reindl, B., Macchetto, F. D., & Panagia, N. 2006, ApJ, 653, 843
Sasselov, D. D., et al. 1997, A&A, 324, 471
Schlegel, D. J., Finkbeiner, D. P., & Davis, M. 1998, ApJ, 500, 525
Schultz, G. V., & Wiemer, W. 1975, A&A, 43, 133
Sills, A., Pinsonneault, M. H., & Terndrup, D. M. 2000, ApJ, 534, 335
Skrutskie, M. F., et al. 2006, AJ, 131, 1163
Sneden, C., Gehrz, R. D., Hackwell, J. A., York, D. G., & Snow, T. P. 1978, ApJ, 223, 168
Soszyński, I., Gieren, W., Pietrzyński, G., Bresolin, F., Kudritzki, R.-P., & Storm, J. 2006, ApJ, 648, 375
Stetson, P. B. 2000, PASP, 112, 925
Storm, J., Carney, B. W., Gieren, W. P., Fouqué, P., Latham, D. W., & Fry, A. M. 2004, A&A, 415, 531
Tammann, G. A., Sandage, A., & Reindl, B. 2003, A&A, 404, 423
Thackeray, A. D., Wesselink, A. J., & Harding, G. A. 1962, MNRAS, 124, 445
Torres, G., & Ribas, I. 2002, ApJ, 567, 1140
Trumpler, R. J. 1921, Lick Observatory Bulletin, 10, 110
Turner, D. G. 1979, PASP, 91, 642
Turner, D. G. 1986, AJ, 92, 111
Turner, D. G., Forbes, D., & Pedreros, M. 1992, AJ, 104, 1132
Turner, D. G., Pedreros, M. H., & Walker, A. R. 1998, AJ, 115, 1958
Udalski, A. 2000, Acta Astronomica, 50, 279
Udalski, A., Pietrzyński, G., Woźniak, P., Szymański, M., Kubiak, M., & Żebruń, K. 1998, ApJ, 509, L25
Udalski, A., Soszyński, I., Szymański, M., Kubiak, M., Pietrzyński, G., Woźniak, P., & Żebruń, K. 1999a, Acta Astronomica, 49, 223
Udalski, A., Szymański, M., Kubiak, M., Pietrzyński, G., Soszyński, I., Woźniak, P., & Żebruń, K. 1999b, Acta Astronomica, 49, 201
van den Bergh, S. 1957, ApJ, 126, 323
van den Bergh, S., & Harris, G. L. H. 1976, ApJ, 208, 765
van Leeuwen, F. 2005, A&A, 439, 805
van Leeuwen, F., & Fantino, E. 2005, A&A, 439, 791
van Leeuwen, F., Feast, M. W., Whitelock, P. A., & Laney, C. D. 2007, MNRAS, 379, 723
Walker, A. R. 1985, MNRAS, 213, 889
Walker, A. R. 1987, South African Astronomical Observatory Circular, 11, 131
Walker, A. R. 1999, in Post-Hipparcos Cosmic Candles, ed. A. Heck & F. Caputo (Dordrecht: Kluwer), 125
Walker, A. R, & Coulson, I. M. 1985, South African Astronomical Observatory Circular, 9, 97
Wallerstein, G. 1957, PASP, 69, 172
Wampler, J., Pesch, P., Hiltner, W. A., & Kraft, R. P. 1961, ApJ, 133, 895
Yong, D., Carney, B. W., Teixera de Almeida, M. L., & Pohl, B. L. 2006, AJ, 131, 2256
Zaritsky, D., Kennicutt, R. C., Jr., & Huchra, J. P. 1994, ApJ, 420, 87